Received: 14 April 2023 | Accepted: 8 August 2023

DOI: 10.1111/jpy.13387

RESEARCH ARTICLE

New branched *Porolithon* species (Corallinales, Rhodophyta) from the Great Barrier Reef, Coral Sea, and Lord Howe Island

So Young Jeong[1] | **Paul W. Gabrielson**[2] | **Jeffery R. Hughey**[3] | **Andrew S. Hoey**[4] | **Tae Oh Cho**[5] | **Muhammad A. Abdul Wahab**[6] | **Guillermo Diaz-Pulido**[7]

[1]Australian Rivers Institute-Coast & Estuaries and Coastal and Marine Research Centre, School of Environment and Science, Nathan Campus, Griffith University, Nathan, Queensland, Australia

[2]Biology Department and Herbarium, University of North Carolina at Chapel Hill, Chapel Hill, North Carolina, USA

[3]Division of Mathematics, Science, and Engineering, Hartnell College, Salinas, California, USA

[4]ARC Centre of Excellence for Coral Reef Studies and College of Science and Engineering, James Cook University, Townsville, Queensland, Australia

[5]Department of Life Science, Chosun University, Gwangju, South Korea

[6]Australian Institute of Marine Science, Townsville, Queensland, Australia

[7]Coastal and Marine Research Centre, School of Environment and Science, Nathan Campus, Griffith University, Nathan, Queensland, Australia

Correspondence
Guillermo Diaz-Pulido, Coastal and Marine Research Centre, School of Environment and Science, Griffith University, Nathan Campus, 170 Kessels Road, Nathan, QLD 4111, Australia.
Email: g.diaz-pulido@griffith.edu.au

Funding information
Australian Biological Resources Study, Grant/Award Number: RG19-35; Australian Institute of Marine Science; Australian Research Council, Grant/Award Number: DP160103071; Great Barrier Reef Foundation; Ministry of Ocean and Fisheries of Korea, Grant/Award Number: 20210469; National Marine Biodiversity Institute of Korea; National Research Foundation of Korea, Grant/Award Number: 2021R1I1A2059577; Private family trust (P.W.G.)

Editor: H. Verbruggen

Abstract

Porolithon is one of the most ecologically important genera of tropical and subtropical crustose (non-geniculate) coralline algae growing abundantly along the shallow margins of coral reefs and functioning to cement reef frameworks. Thalli of branched, fruticose *Porolithon* specimens from the Indo-Pacific Ocean traditionally have been called *P. gardineri*, while massive, columnar forms have been called *P. craspedium*. Sequence comparisons of the *rbc*L gene both from type specimens of *P. gardineri* and *P. craspedium* and from field-collected specimens demonstrate that neither species is present in east Australia and instead resolve into four unique genetic lineages. *Porolithon howensis* sp. nov. forms columnar protuberances and loosely attached margins and occurs predominantly at Lord Howe Island; *P. lobulatum* sp. nov. has fruticose to clavate forms and free margins that are lobed and occurs in the Coral Sea and on the Great Barrier Reef (GBR); *P. parvulum* sp. nov. has short (<2 cm), unbranched protuberances and attached margins and is restricted to the central and southern GBR; and *P. pinnaculum* sp. nov. has a mountain-like, columnar morphology and occurs on oceanic Coral Sea reefs. A *rbc*L gene sequence of the isotype of *P. castellum* demonstrates it is a different species from other columnar species. In addition to the diagnostic *rbc*L and *psb*A marker sequences, the four new species may be distinguished by a combination of features including thallus growth form, margin shape (attached or unattached), and medullary system (coaxial or plumose).

Abbreviations: BP, bootstrap; BPP, Bayesian posterior probability; CCA, Crustose, non-geniculate coralline algae; GBR, Great Barrier Reef; GTR, General time reversible model; I, proportion of invariable sites; ML, maximum likelihood; *psb*A, plastid-encoded gene of photosystem II reaction center D1 protein gene; RAxML, randomized accelerated maximum likelihood; *rbc*L, ribulose-1,5-bisphosphate carboxylase/oxygenase large subunit.

Porolithon species, because of their ecological importance and sensitivity to ocean acidification, need urgent documentation of their taxonomic diversity.

KEYWORDS
crustose coralline algae, morpho-anatomy, non-geniculate coralline algae, phylogeny, *Porolithon castellum*, *Porolithon craspedium*, *Porolithon gardineri*, *psb*A, *rbc*L, taxonomy, type specimen sequencing

INTRODUCTION

Crustose, non-geniculate coralline algae (CCA) are calcifying red algae that are important components of coral reefs and both rhodolith and maerl beds (Adey, 1978b; Rindi et al., 2019; Teichert et al., 2020). These CCA deposit calcium carbonate in their cell walls and through this process of calcification contribute to coral reef growth, reinforcing the reef framework, filling cracks, and cementing (Littler & Doty, 1975; Nash et al., 2019). They also promote larval settlement of key benthic invertebrates, including corals, thus potentially playing an important role in coral population recovery and reef resilience (Birkeland et al., 2021; Daume et al., 1999; Doropoulos et al., 2016; Harrington et al., 2004; Jorissen et al., 2021). Further, many CCA provide habitat for numerous marine organisms (Adey, 1998; Bjork et al., 1995; Bosence, 1983; Diaz-Pulido et al., 2007; Heyward & Negri, 1999; O'Leary et al., 2017; Payri & Cabioch, 2004). Among the tropical CCA, the genus *Porolithon* is one of the most abundant in shallow water environments and is a significant contributor to reef building (Adey, 1978a; Dechnik et al., 2017; Diaz-Pulido et al., 2014; Littler & Doty, 1975).

Porolithon differs from other members of the subfamily Metagoniolithoideae (sensu Richards et al., 2021; Corallinales) by possessing densely packed, pustulate trichocytes in horizontal fields (without intervening vegetative cells between them) clearly visible on a surface view (Maneveldt & Keats, 2014, 2016; Richards et al., 2021). There are 16 species of *Porolithon* currently recognized worldwide, all with a predominantly tropical to subtropical distribution (Guiry & Guiry, 2023).

Porolithon species from the Indo-Pacific Ocean can be artificially grouped into two categories based on their external morphology (form or habit; S. Jeong & G. Diaz-Pulido, personal observation). One group comprises species with smooth, unbranched thalli, and a recent genomic study revealed a wealth of previously undocumented diversity (Gabrielson et al., 2018). DNA sequence data showed that an apparently widespread species, *P. onkodes*, actually comprised over 20 "cryptic" species (i.e., species that look very similar but are genetically distinct; Struck et al., 2018). This finding of cryptic species reinforced the importance of using DNA sequences for species diversity studies in this genus. The second group comprises species with branched thalli, that is, having numerous elongated protuberances or vertical columns. In the Indo-Pacific Ocean, branched *Porolithon* specimens have been variously referred to as either one species, *P. gardineri* (type locality: Coetivy Reef, Chagos Archipelago, Mauritius), or two species, *P. craspedium* (type locality: Onotoa, Gilbert Islands, Kiribati) and *P. gardineri* (Dawson, 1957; Kato et al., 2011; Littler & Littler, 2013; Payri & N'Yeurt, 1997; Santelices & Abbott, 1987; South & Skelton, 2003; Taylor, 1950; Tsuda, 2003; Tsuda & Fisher, 2012; Tsuda & Walsh, 2013). A partial *rbc*L gene sequence from the type specimen of *P. gardineri* was analyzed recently and shown to be distinct from other species of *Porolithon*, including *P. coarctatum,* which had been considered its synonym (Richards et al., 2021). In the central eastern Pacific Ocean, *P. castellum* (type locality: Isla del Caño, Costa Rica) has been reported in shallow intertidal areas and the shallow subtidal zone (Dawson, 1960).

As part of an effort to document the diversity of coralline algae from the tropical and subtropical regions of eastern Australia, we collected 58 branched *Porolithon* specimens that resembled the columnar *P. castellum* and *P. craspedium* and the shorter branched *P. gardineri* from along more than 2300 km of coast on the Great Barrier Reef (GBR), encompassing a variety of habitats across the Australian continental shelf, from inshore to outer reefs of the GBR and from remote oceanic atolls in the Coral Sea Marine Park. We extended our collection effort to include Lord Howe Island (31°33′19.08″ S, 159°4′55.56″ E), the southernmost true coral reef in the world. The collected specimens showed considerable variability in branching patterns and the height and thickness of protuberances and vertical columns. Given the documented case of cryptic speciation in the smooth *Porolithon* group (Gabrielson et al., 2018) and to reliably distinguish individual species, we analyzed chloroplast-encoded *rbc*L and *psb*A gene sequences and compared morpho-anatomical features among collected specimens. Importantly, the isotype of *P. castellum* and the holotype of *P. craspedium* were sequenced. Based on the two sequenced genes, as well as morpho-anatomical characters, four new *Porolithon* species are described from the east coast of Australia (the GBR, Coral Sea, and Lord Howe Island).

MATERIALS AND METHODS

Specimen collections

A total of 58 fresh specimens of branched *Porolithon* were collected by SCUBA at depths between 2 and 9 m using a hammer and chisel, from 15 localities in the GBR, Coral Sea, and Lord Howe Island, Australia (Figure 1; Table S1 in the Supporting Information), under the Great Barrier Reef Marine Park Authority Permit G18/41291.1, G18/40881.1, G21/45348.1, the Australian Government Department of the Environment Permit AU-COM2022-542 (Coral Sea samples), and Department of Primary Industries Marine Parks permit LHIMP/R/18011/12092018 (Lord Howe Island samples). Specimens were photographed underwater (Canon PowerShot G1X Mark II in a WP-DC53 waterproof case), labeled, air-dried, and then preserved with silica gel in resealable polyprophylene bags. Holotypes and isotypes were deposited at the Queensland Herbarium (BRI). Further voucher specimens were lodged in the Coral Reef Algae Laboratory (DP) at Griffith University (Table S1). Type material of *P. castellum* (UC 201237) and *P. craspedium* (TRH A27-1566) were borrowed for study. Herbarium acronyms followed Thiers (2023, continuously updated).

DNA extractions, PCR amplification, and sequencing

Field collected samples were carefully cleaned with a brush and forceps under a dissecting microscope to remove epiphytes and endophytes. Tissue for DNA was collected by scraping the thallus surface with a single edge razor blade. DNA extractions of the type specimens of *Porolithon castellum* and *P. craspedium* were done by JRH following the precautionary guidelines of Hughey and Gabrielson (2012). Amplification of the *rbc*L gene sequences from type specimens used the primer pair F1150Cor-R1460 (3' end) and the PCR protocol outlined in Hernandez-Kantun et al. (2015). DNA extractions and PCR of field-collected specimens followed Jeong et al. (2021). Amplifications and sequencing of the field-collected material by SYJ used three primer sets, F762/R*rbc*Start or F993/R*rbc*Start or F1150/R*rbc*Start (Freshwater & Rueness, 1994), for *rbc*L and two primer sets, either *psb*AF1/*psb*AR2 or *psb*AF1/*psb*A600R (Yoon et al., 2002), for *psb*A. The PCR amplification consisted of an initial denaturation for 2 min at 95°C, followed by 40 cycles of 20 s denaturation at 95°C, annealing for 40 s at 40°C, and extension for 1 min at 72°C. The final extension step was carried out at 72°C for 5 min. These primers were also used in cycle sequencing. Sequencing of specimens extracted and amplified by JRH was performed by Functional Biosciences, Inc., Madison, Wisconsin, and by SYJ by

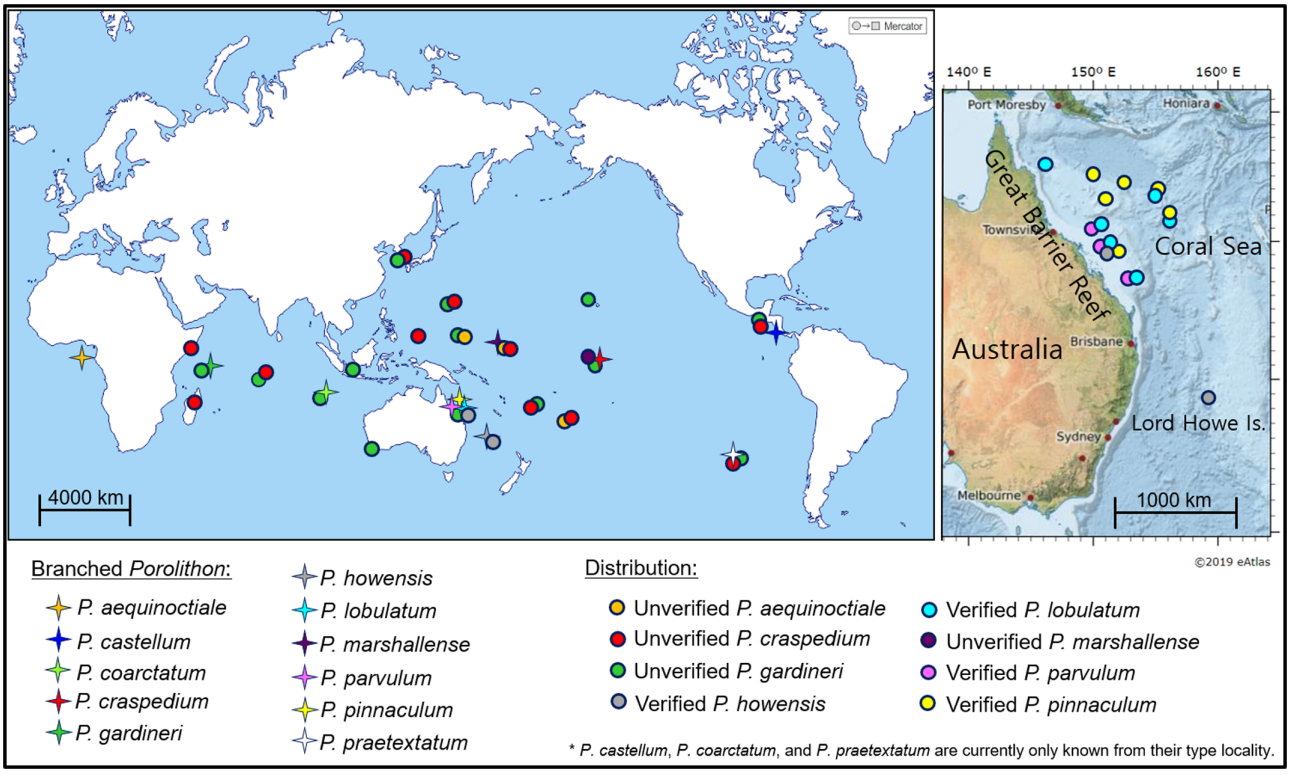

FIGURE 1 Type localities of branched *Porolithon* species (✧) including their verified/unverified geographic distributions (○).

Macrogen, Seoul, South Korea. Sequences were deposited in GenBank (Table S1).

Sequence and phylogenetic analyses

A dataset of *rbc*L and *psb*A gene sequences was analyzed, including newly generated sequences, from taxa in the subfamily Metagoniolithoideae (sensu Richards et al., 2021) to resolve phylogenetic relationships. Sequences from *Adeylithon bosencei* and *Hydrolithon* cf. "*reinboldii*" (=*H. boergesenii*) were selected for the *rbc*L gene as outgroups, and *A. bosencei*, *H. boergesenii*, and *H*. "*reinboldii*" (=*H. boergesenii*) were selected for the *psb*A gene as outgroups. Datasets were aligned using ClustalW (Thompson et al., 1994) and manually corrected using MEGA7 (Kumar et al., 2016). PartitionFinder 2 (Lanfear et al., 2016) was used to determine the best partition scheme and model of evolution as implemented by RAxML. For maximum likelihood (ML) analysis, the general time reversible (GTR) + G model was selected as the best-fit model for *rbc*L, whereas the GTR + G + I model was chosen for the *psb*A data with 1000 bootstrap (BP) replicates using RAxMLGUI v1.5 (Silvestro & Michalak, 2012; Stamatakis, 2006; Stamatakis et al., 2008). Bayesian analysis was performed using MrBayes 3.1.2 (Huelsenbeck & Ronquist, 2001; Ronquist & Huelsenbeck, 2003). Markov chain Monte Carlo runs were carried out for 2 million generations, each with one cold chain and three heated chains, using the GTR + G and GTR + G + I evolutionary models, with sampling and occurring every 1000 generations. Summary trees were generated using a burn-in of 25%.

Morpho-anatomical observations

Only DNA confirmed specimens were used for the morpho-anatomical studies. External morphology was observed under a stereomicroscope (Olympus SZX16), and photos were taken using an Olympus DP72 digital camera. For anatomical observations, silica-dried samples were first decalcified in 0.6 M nitric acid until the gas bubbles ceased forming, then rinsed with distilled water and stained using aniline blue for 30–60 min. Specimens were immersed in 30%, 70%, 90%, and 100% ethanol solutions, respectively, for a minimum of 60 min each to displace any water and acid in the specimens following Maneveldt and Keats (2014). Thereafter, each specimen was removed from the 100% ethanol and allowed to air dry for no more than a few seconds. Specimens were then immersed in White Resin (Electron Microscopy Sciences) overnight until completely infiltrated. The specimens were oriented in the mold and a hardening solution LR White accelerator (Electron Microscopy Sciences) was added to the same mold. The mold was then left at room temperature for at least for 4 h to stabilize the sample and prevent bubbles from forming in the resin block. Gelling of the hardener usually occurred in 1–2 h on the hot plate. Thallus sections, 4–10 μm thick, were prepared using a rotary microtome (Leica RM2125 RTS). Sections were then stained (again) with aniline blue and toluidine blue (Electron Microscopy Sciences) and mounted onto microscope slides. Permanent slides were mounted in Omnimount (Electron Microscopy Sciences). Micrographs were taken using a compound light microscope (Olympus BX53) equipped with an Olympus DP72 digital camera.

For SEM, selected fragments of dried samples were mounted on aluminum stubs using double-sided adhesive carbon tape (Nisshin EM) and coated with 18–20 nm of gold using a digital ion sputter coater (SPR-20, COXEM). Samples were examined in a COXEM EM-30 PLUS SEM (Mini SEM; COXEM) at an accelerating voltage of 15 kV at Chosun University, Korea.

Terminology and measurements

Thallus anatomical and morphological terminology followed Chamberlain (1990) and Woelkerling (1993), respectively. For cell measurements, length denotes the distance between primary pit connections, and diameter denotes the maximum width of the cell lumen at right angles to length. Conceptacle measurements followed Adey and Adey (1973). The determination and presentation (i.e., range and not averages, with standard deviations/errors) of all measurements followed Maneveldt et al. (2017).

RESULTS

Sequence data

A total of 100 gene sequences were newly generated in the present study: 50 *rbc*L (118–654 bp) and 50 *psb*A (225–840 bp; Table S1). Phylogenetic trees inferred from the *rbc*L and *psb*A gene sequences showed similar topologies in ML analyses and Bayesian inference (Figures 2 and 3). In both the *rbc*L and *psb*A trees, a monophyletic *Porolithon* is strongly supported in the ML analyses (97/1.00 for BP and Bayesian posterior probability [BPP], respectively, in *rbc*L, 99/1.00 in *psb*A). The partial *rbc*L gene sequences (118 bp) generated from the type specimens of two branched *Porolithon* species, *P. castellum* and *P. craspedium*, were resolved in a clade with *P. onkodes*, the generitype of *Porolithon* (Figure 2). The two type sequences differed by

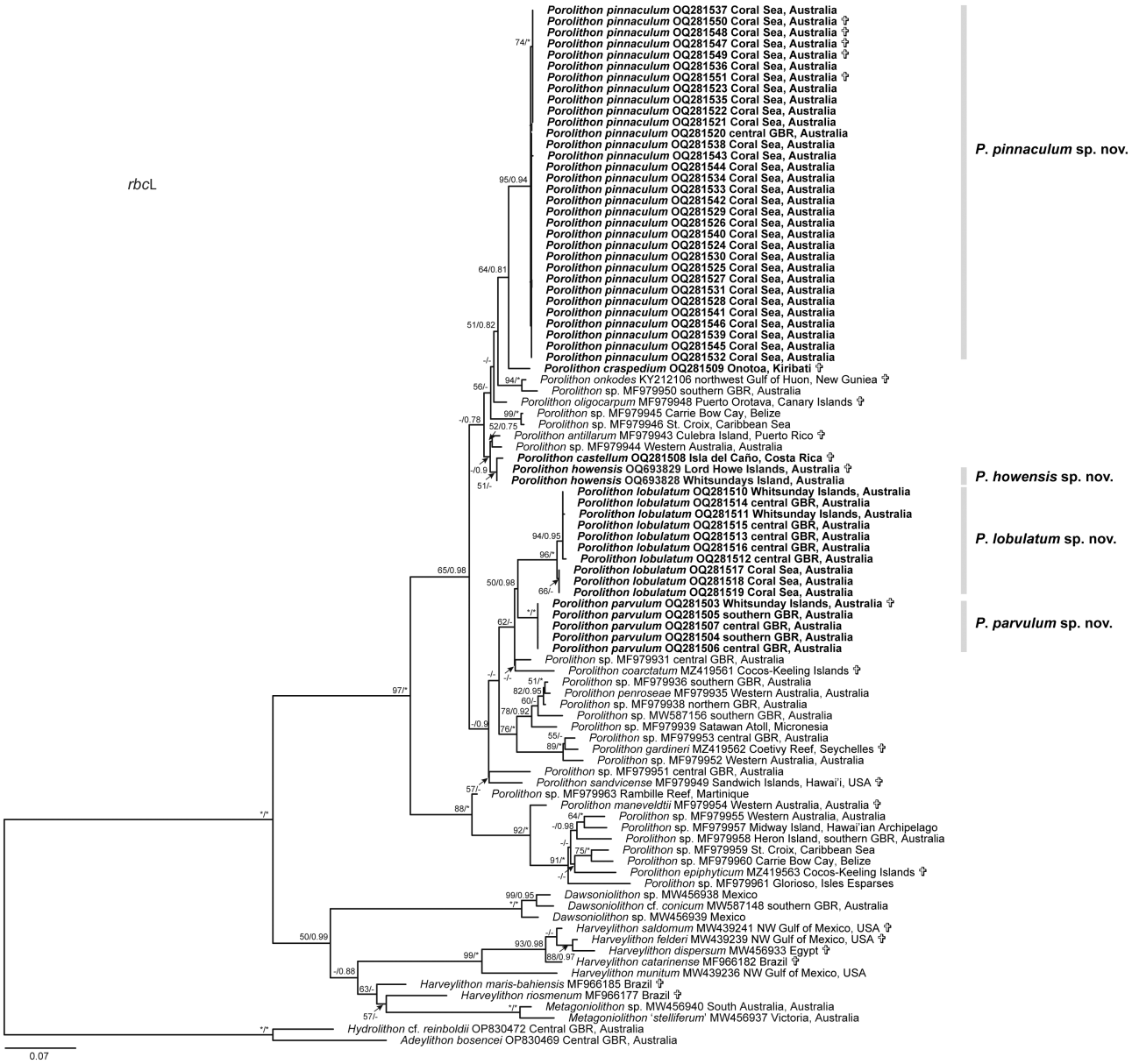

FIGURE 2 Phylogenetic tree based on maximum likelihood (ML) analysis of *rbc*L gene sequences. Values above branches denote maximum likelihood bootstrap values (BP) in % > 50/Bayesian posterior probabilities (BPP) > 0.75. BP values <50% and BPP values <0.75 are indicated by hyphens (–). BP values of 100% and BPP values of 1.00 are indicated by asterisks (*). Sequences obtained from this study are in bold. Sequences obtained from type materials are indicated by the cross (✞). Each sequence presented with species name, GenBank accession number, and geographic location.

10 bp, a sequence divergence of over 8.5%, and they were phylogenetically distant from each other within *Porolithon* (Figure 2). For both the *rbc*L and *psb*A gene datasets, the new field-collected samples of *P. howensis* sp. nov., *P. lobulatum* sp. nov., *P. parvulum* sp. nov., and *P. pinnaculum* sp. nov. (described hereunder) were nested in a clade along with other specimens ascribed to *Porolithon* and distinguished from congeners.

In the *rbc*L gene tree, *Porolithon howensis* sp. nov. was a sister species to isotype of *P. castellum* (Figure 2) with sequence divergence values of 0.7%. Interspecific *rbc*L gene sequence divergences between *P. howensis* sp. nov. and type specimens of *P. craspedium* and *P. gardineri* were 7.6% and 7.1%–8%, respectively. Sequence divergences between *P. howensis* sp. nov. and *P. parvulum* sp. nov. were 6.9%–7.7% for *rbc*L and 5.1%–5.5% for *psb*A; between *P. howensis* and *P. lobulatum* sp. nov., they were 7.1%–9.4% for *rbc*L and 5.2%–7.1% for *psb*A; between *P. howensis* and *P. pinnaculum* sp. nov., they were 5.1%–6.2% for *rbc*L and 2.9%–3.3% for *psb*A.

The *rbc*L gene sequence divergence between *Porolithon parvulum* sp. nov. and the lectotype of *P. gardineri* was 8.4%, and between *P. lobulatum* sp. nov. and the lectotype of *P. gardineri*, it was 5.8%–9.9%.

FIGURE 3 Phylogenetic tree based on maximum likelihood (ML) analysis of *psb*A gene sequences. Values above branches denote maximum likelihood bootstrap values (BP) in % > 50/Bayesian posterior probabilities (BPP) > 0.75. BP values <50% and BPP values <0.75 are indicated by hyphens (–). BP values of 100% and BPP values of 1.00 are indicated by asterisks (*). Sequences obtained from this study are in bold. Sequences obtained from type materials are indicated by the cross (✞). Each sequence presented with species name, GenBank accession number, and geographic location.

Sequence divergence values between *P. parvulum* sp. nov. and *P. lobulatum* sp. nov. were 3.9%–6.5% for *rbc*L and 3.9%–4.5% for *psb*A. In both *rbc*L and *psb*A gene analyses, *P. parvulum* sp. nov. was a sister taxon to *P. lobulatum* sp. nov., although the supporting value for BP was low in the *rbc*L tree (50/0.98 in *rbc*L, 97/1.00 in *psb*A).

In the *rbc*L gene tree, *Porolithon pinnaculum* sp. nov. was a sister species to *P. craspedium* (Figure 2), with sequence divergence values of 5.1%–5.9%. Interspecific *rbc*L sequence divergences between *P. pinnaculum* sp. nov. and type specimens of *P. castellum* and *P. gardineri* were 7.4%–8.3% and 8.5%–9.1%, respectively. Sequence divergences between *P. pinnaculum* sp. nov. and *P. parvulum* sp. nov. were 6.8%–11.2% for *rbc*L and 5.4%–5.8% for *psb*A; between *P. pinnaculum* and *P. lobulatum* sp. nov., they were 7.2%–9.1% for *rbc*L and 5.7%–6.3% for *psb*A.

Taxonomic results

Based on the phylogenetic analyses of *rbc*L and *psb*A gene sequences and morpho-anatomical observations, four new species of branching *Porolithon* are proposed: *P. howensis* sp. nov., *P. lobulatum* sp. nov., *P. parvulum* sp. nov., and *P. pinnaculum* sp. nov.

Porolithon howensis S.Y.Jeong & G.Diaz-Pulido **sp. nov**. (Figures 4 and 5)

Holotype (designated here): BRI1040964, 15.xii.2010, reef front; 5–7 m deep, *leg*. Guillermo Diaz-Pulido; GenBank accessions: *rbc*L: OQ693829, *psb*A: OQ693827.

Type locality: North Passage (spurs & grooves zone), Lord Howe Island, New South Wales, Australia (31°31.26′ S, 159°02.49′ E).

Etymology: The epithet *howensis* refers to the type locality of Lord Howe Island in New South Wales, Australia.

Additional specimens examined: confirmed by DNA sequencing (Table S1).

Habitat and geographic distribution: *Porolithon howensis* occurs in shallow water coral reef habitats, particularly reef fronts between depths of 4 and 7 m in the spurs and grooves zone in Lord Howe Island, Australia. Specimens grow attached to the carbonate substrates. One specimen also confirmed by DNA sequencing was found in the central GBR (Tideway Reef, 19°59.5′ S, 149°45.3′ E) in the outer reefs of the Whitsunday region, Australia.

Description. Plants non-geniculate, lumpy, with short terete, bearing individual to fused protuberances (Figure 4a,b). Protuberances cylindrical, robust, thick, 8–25 mm long, 6–9 mm wide, with rounded to flattened apex (Figure 5a), but branches, when fused, loose cylindrical shape. Living thalli pearl white (HTML color code #F8F6F0), chalky in color. Thallus margins loosely attached, but no free margins. Surface texture smooth, matte, and granular due to presence of abundant tightly packed, postulate, horizontal trichocyte fields (Figure 5b,c).

Vegetative anatomy: Cortical cells square to rectangular, 4–13 μm long, 4–7 μm wide. Cell fusions abundant; secondary pit connections not observed. Trichocyte fields 116–142 μm in external diameter, 7–12 trichocytes grouped in vertical section, often overgrown and buried in horizontal fields. Individual trichocytes rectangular to elongate, tightly packed and horizontally arranged without intervening cortical cells, 9–20 μm long, 13–20 μm wide, and buried (Table 1; Figure 5c). Haustoria not observed.

Reproductive anatomy: Gametangial plants not found. Tetrasporangial conceptacles uniporate, raised above surrounding thallus surface (Figure 5d), 66–75 μm in external diameter. Conceptacle chambers elliptical to bean-shaped, 186–197 μm in diameter, 51–67 μm in height, with the roof 22–39 μm (7–11 cells; including epithallial cell) thick (Figure 5e). Conceptacle floor located 10–15 cell layers below epithallus. Central columella not observed. Tetrasporangial conceptacles buried in the thallus; infilled conceptacles not observed. Data on measured reproductive characters summarized in Table 1.

Porolithon lobulatum S.Y.Jeong & G.Diaz-Pulido **sp. nov.** (Figures 4 and 6).

Holotype (designated here): BRI1040965, 02.iii.2012, growing attached to dead coral, reef crest; 3–4 m deep, *leg*. Guillermo Diaz-Pulido; GenBank accessions: *psb*A: OQ281463.

Type locality: Libby's lair, Heron Island, southern GBR, Australia (23°26.066′ S, 151°56.183′ E).

Etymology: The epithet *lobulatum* refers to the thallus having free margins that are unattached and lobed.

Additional specimens examined: all confirmed by DNA sequencing (Table S1).

Habitat and geographic distribution: *Porolithon lobulatum* occurs in shallow water coral reef habitats, particularly reef crests and upper reef slopes between depths of 2 and 9 m. Specimens grow attached to the surface of coral skeletons and other carbonate substrates. Specimens confirmed by DNA sequencing are widely distributed along the Australian GBR, including the northern (Yonge Reef, 14°35.883′ S, 145°37.45′ E), an outer reef near Lizard Island, central (Joist Reef, 19°27.9′ S, 149°38.566′ E), in the outer reefs of the Whitsunday region and Davies Reef (18°49.433′ S, 147°39.05′ E), and southern (Heron Island) sections, and in the Coral Sea in Australia: Marion Reef (19°11.233′ S, 152°17.283′ E), Lihou Reef (17°26.6′ S, 151°34.916′ E), and Diamond Islets (17°31.2′ S, 150°17.3′ E).

Description. Plants non-geniculate, fruticose, with short terete, loosely dichotomously to multiple and densely branched rounded clumps, bearing short individual to fused protuberances (Figure 4c–h). Protuberances irregular, cylindrical to clavate, 4–24 mm long, 3–10 mm wide, with rounded to concave to capitate apex (Figure 6a). Living thalli light to dark pink in color. Thallus margins free, entirely to lobed (Figure 6b), but lack orbital ridges. Surface texture smooth, matte, and granular due to presence of abundant tightly packed, postulate, horizontal trichocyte fields (Figure 6c).

Vegetative anatomy: Thalli dorsiventrally organized, monomerous with medullary filaments predominately coaxial in crustose areas (Figure 6d). Medullary cells square to rectangular, 8–24 μm long, 7–13 μm wide. Cortical cells square to rectangular, 2–27 μm long, 3–13 μm wide. Subepithallial initials (intercalary meristematic cells) squarish with rounded corners, 2–14 μm in length, 4–11 μm in diameter (Figure 6e). Epithallus one to three layers of squat to elliptical cells, 1–3 μm long, 4–10 μm wide (Figure 6e). Cell fusions abundant (Figure 6e); secondary pit connections not observed. Trichocyte fields 47–175 μm in external diameter, 4–13 trichocytes grouped in vertical section, often overgrown and buried in horizontal fields (Figure 6f). Individual

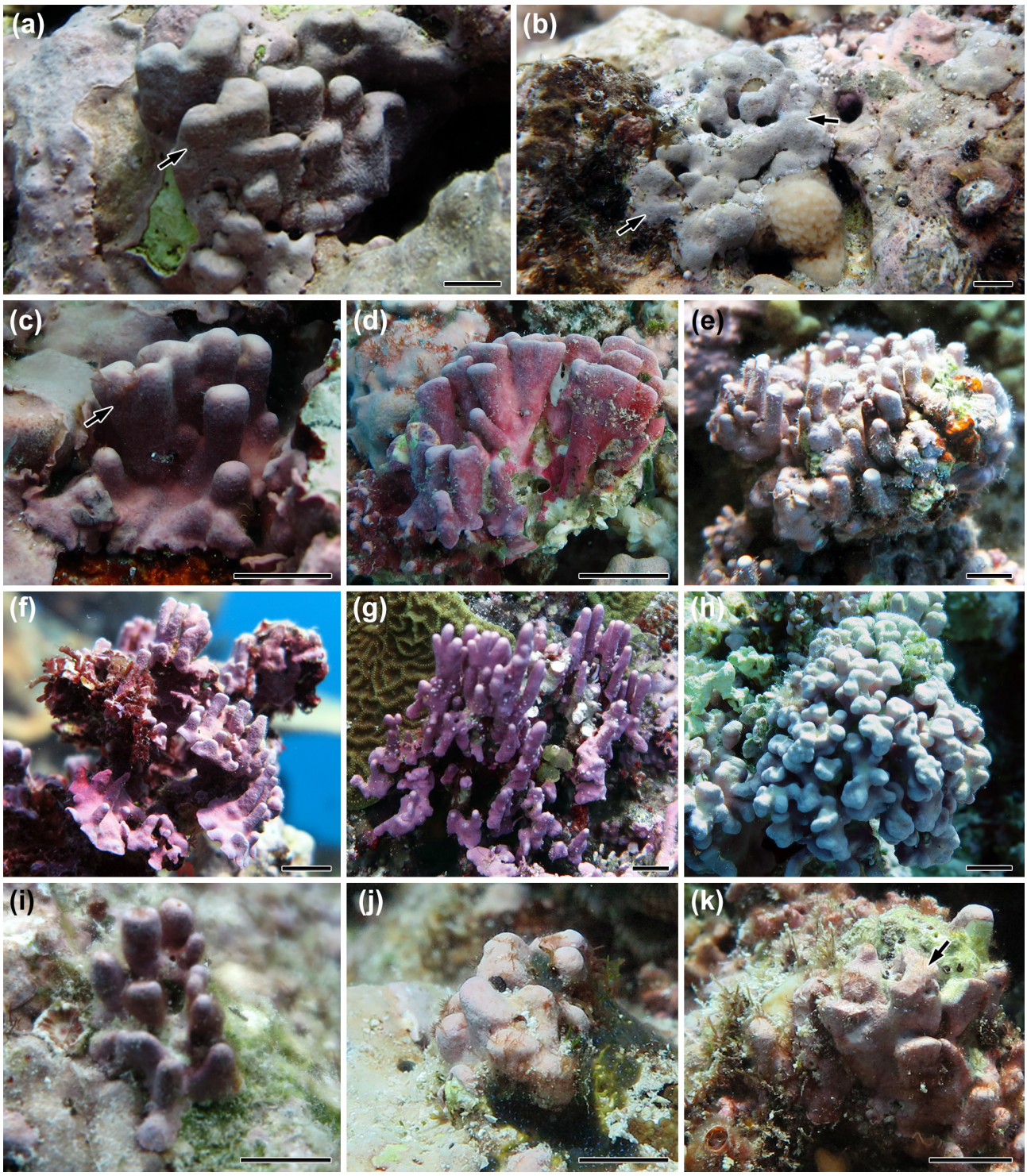

FIGURE 4 Field photos showing external morphological variation of *Porolithon howensis* (a and b), *P. lobulatum* (c–h), and *P. parvulum* (i–k). (a) Thallus with short, robust, fused columnar branches (arrow; BRI1040964). (b) Initial thallus growth stage with lumpy protuberances (arrows; DP-1982). (c) Thallus with both short terete, unfused branches and fused columnar branches (arrow; DP-1110). (d) Thallus with compressed and fused, fan-shaped branches (BRI1040965). (e) Thallus with terete, mostly unbranched branches (DP-2461). (f) Thallus with free margins (DP-2459). (g) Thallus with slender, terete, mostly unfused protuberances (DP-2618-1). (H) Heavily branched thallus with reniform, partly fused shaped branch apices (DP-2625-1). (i) Thallus with short terete, mostly unfused branches (BRI1040960). (j and k) Thallus with fused branches (DP-2248, DP-2249 [arrow], respectively). Scale bars = 1 cm.

trichocytes rectangular to elongate, tightly packed and horizontally arranged without intervening cortical cells, 18–40 μm long, 8–16 μm wide, and buried (Table 1; Figure 6f). Haustoria not observed.

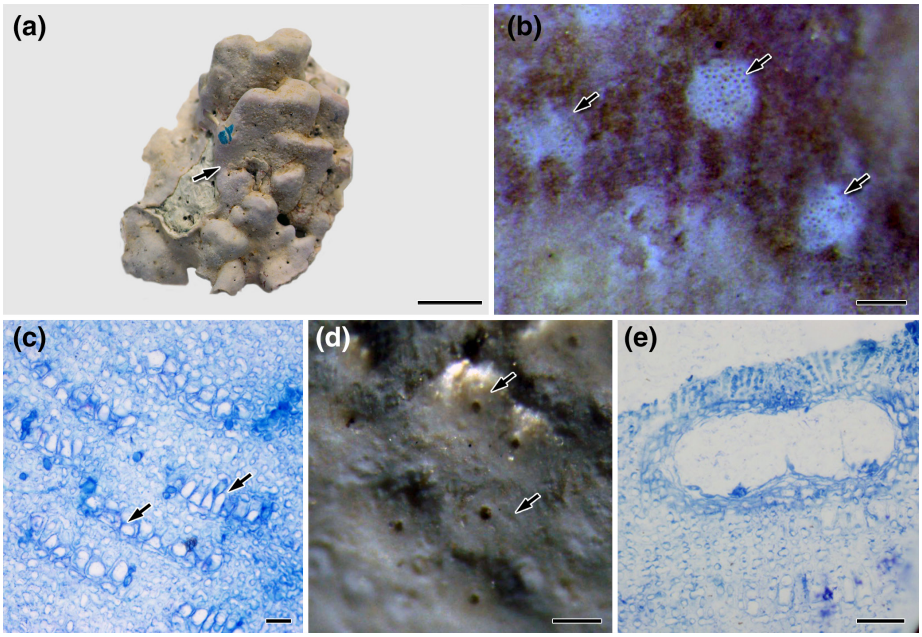

FIGURE 5 Vegetative and sporangial morpho-anatomy of *Porolithon howensis*. (a) Holotype specimen (arrow; BRI1040964). Scale bar = 1 cm. (b) Surface view showing trichocyte fields (arrows; BRI1040964). Scale bar = 500 μm. (c) Vertical section through the thallus showing buried trichocyte fields (arrows; DP-1982). Note the absence of vegetative filaments between trichocyte megacells. Scale bar = 20 μm. (d) Surface view showing sporangial conceptacles (arrows; DP-1982). Scale bar = 50 μm. (e) Vertical section through a sporangial conceptacle showing elliptical-shaped chamber (DP-1982). Scale bar = 20 μm.

Reproductive anatomy: Gametangial plants monoecious (Figure 6h). Carpogonial conceptacles not seen. Uniporate carposporangial conceptacles raised to mound-shaped (mostly; Figure 6g), 147–325 μm in external diameter, 42–75 μm in external height above thallus surface or flush to slightly sunken in 24–48 μm depth below the thallus. Carposporangial conceptacle chambers elliptical, 153–226 μm in diameter, 45–80 μm in height, with the roof 35–53 μm (5–10 cells; incl. epithallial cell) thick (Figure 6h; arrow). Conceptacle floor located 11–14 cell layers below epithallus. Continuous central fusion cell narrow and thick (discoid), with gonimoblast filaments borne peripherally. Gonimoblast filaments three to five cells long including terminal carposporangium (Figure 6i). Uniporate male (spermatangial) conceptacles small, flush to slightly raised above surrounding thallus surface, 8–16 μm in external height above thallus. Male conceptacle chambers triangular to boat-shaped (Figure 6h; arrowhead), 69–85 μm in diameter, 13–54 μm in height, with roof 29–41 μm (6–11 cells; including epithallial cell) thick. Simple spermatangial systems borne only on floor of conceptacle chamber (Figure 6j,k). Both female and male conceptacles often buried in the thallus.

Tetrasporangial conceptacles uniporate, raised above surrounding thallus surface (Figure 6l), 101–291 μm in external diameter, 18–58 μm in external height above surrounding thallus surface. Conceptacle chambers elliptical to bean-shaped, 127–197 μm in diameter, 52–103 μm in height, with the roof 27–61 μm (6–13 cells; incl. epithallial cell) thick (Figure 6m). Conceptacle floor located 10–15 cell layers below epithallus. Pore canals 24–42 μm in length, 16–34 μm in diameter. Pore canal filaments orientated perpendicular and not projecting into pore. A ring of enlarged cells lines the base of the pore canal (Figure 6n). Tetrasporangia zonately divided, 22–73 μm long, 4–29 μm wide (Figure 6m). Central columella not observed. Tetrasporangial conceptacles buried in the thallus; infilled conceptacles not observed. Data on measured reproductive characters summarized in Table 1.

Porolithon parvulum S.Y.Jeong & G.Diaz-Pulido **sp. nov.** (Figures 4 and 7).

Holotype (designated here): BRI1040960, 5.iii.2019, growing attached to dead coral, 4 m deep, *leg*. Guillermo Diaz-Pulido; GenBank accessions: *rbc*L: OQ281503, *psb*A: OQ281455.

Type locality: Ross Reef (Whitsunday region), central GBR, Australia (15°52.25′ S, 149°34.933′ E).

Etymology: The epithet *parvulum* is explained by the word *parvulus* of Latin origin meaning small. The specific epithet refers to the thallus having short protuberances compared to other branched congeneric.

Additional specimens examined: all confirmed by DNA sequencing (Table S1).

Habitat and geographic distribution: *Porolithon parvulum* occurs in shallow water coral reef environments, particularly on reef crests and on upper reef slopes 3–6 m deep. Specimens grow attached to the surface of coral skeletons and other carbonate substrates. Specimens

TABLE 1 Comparison of morpho-anatomical features among branched *Porolithon* species (L = length; D = diameter; ND = No data).

Characters	*P. howensis* sp. nov.	*P. lobulatum* sp. nov.	*P. parvulum* sp. nov.	*P. pinnaculum* sp. nov.	*P. aequinoctiale* holotype
Distribution	Central GBR (Whitsunday region) to Lord Howe Island, Australia[a]	Northern to southern GBR (Lizard Is, Heron Is, Davies Reef, Whitsunday region), Coral Sea, Australia[a]	Central to southern GBR (Davies Reef, Whitsunday region, Heron Is), Australia[a]	Central GBR (Davies Reef), Coral Sea, Australia[a]	São Tomé, Rotas Island[a], Micronesia, French Polynesia, Marsahall Islands[b]
Growth form	Lumpy with short terete, bearing cylindrical, robust thick vertical columns	Fruticose, with narrow terete, branches irregular (simple to heavily, dichotomously branched, clavate)	Short terete, mostly unbranched (simple)	Massive, mountain-like, bearing broad individual to fused vertical columns, imbricate	Fruticose, with narrow terete, loosely dichotomously branched, unfused protuberances
Branch fusions	Present	Present	Mostly absent	Present	ND
Branch Apex	Rounded to flattened	Rounded to concave to capitate	Rounded to flattened, slightly concave	Pointed to rounded to flattened, bifurcated	ND
Individual protuberances dimensions	L: 8–25 mm; D: 6–9 mm	L: 4–24 mm; D: 3–10 mm	L: 3–15 mm; D: 3–9 mm	L: 11–97 mm; D: 4–34 mm	L: 3.5 mm; D: 2.5 mm
Margin	Loosely attached, but no free margins	Free margins	Firmly adherent	Firmly adherent or loosely attached, but no free margins	Adherent, lacked orbital ridges
Thallus construction in crustose portions	ND	Monomerous and coaxial	Monomerous and plumose	Monomerous and plumose	Monomerous and plumose
Trichocyte field external diameter (μm)	116–142	47–175	69–148	93–173	ND
Mature tetrasporangial conceptacle chamber diameter (μm)	186–197	127–197	138–228	160–203	ND
References	This study	This study	This study	This study	Foslie (1909), Maneveldt (2005), Maneveldt and Keats (2016)

[a]Original type locality or the distribution confirmed by DNA sequencing.
[b]Based on records from the literature: need to be confirmed by DNA sequencing.

confirmed by DNA sequencing are known from the central (Ross Reef, 15°52.25′ S, 149°34.933′ E, and Stucco Reef, 19°33.316′ S, 149°35.85′ E, in the outer reefs of the Whitsunday region, and Davies Reef, 18°49.433′ S, 147°39.05′ E, off Townsville) and southern (Heron Island) GBR, Australia.

Description. Plants non-geniculate, with short individual to fused protuberances or branches (Figure 4i–k). Protuberances mostly cylindrical (terete), mostly simple (unbranched), 3–15 mm long, 3–9 mm wide, with rounded to flat to slightly concave apices (Figure 7a). Living thalli pink in color. Thallus margins

P. castellum **holotype, isotype**	***P. craspedium*** **holotype**	***P. coarctatum*** **holotype**	***P. gardineri*** **Lectotype**	***P. marshallense*** **holotype, isotype**	***P. praetextatun*** **holotype**
Isla del Caño, Costa Rica[a]	Onotoa, Kiribati[a], Chile, Fiji, French Polynesia, Marshall Islands[b]	Cocos (Keeling) Islands[a]	Coetivy Reef, Chagos Archipelago, Seychelles[a], Chile, Australia, Hawaii, El Salvador, Indonesia, Korea, Polynesia, Micronesia, Guam[b]	Kabella Island, Rongelap Atoll, Marshall Island[a], Line Islands[b]	Chile (Easter Island)[a]
Massive and pinnacled, bearing broad individual to fused columnar protuberances	Massive and mountain-like, bearing broad individual to fused vertical columns	Fruticose, with numerous tightly packed, terete, finely dichotomously branched, unfused protuberances	Fruticose, with narrow terete, loosely dichotomously branched	Cushion-shaped to hemispherical, fruticose with narrow terete, loosely dichotomously branched	Fruticose bearing narrow terete, loosely dichotomously branched, unfused protuberances
Present	Present	ND	Mostly absent	Mostly absent	ND
ND	ND	ND	ND	Blunt	Taper to bluntly pointed
L: 40–60 mm; D: 20–23 mm	ND	L: 16 mm; D: 3 mm	L: 28–50 mm; D: 13–40 mm	L: 30 mm; D: 6 mm	L: 15 mm; D: 3 mm
Free margins, lack orbital ridges	Free margins, lack orbital ridges	ND	Free margins, lack orbital ridges	Free to adherent, and entirely Free margins, lack orbital ridges	ND
Monomerous and plumose	Monomerous and plumose	Monomerous and plumose	Monomerous and plumose	Monomerous and plumose	Monomerous and plumose
ND	ND	ND	ND	ND	ND
200–285	185–250	190–225	160–290	165–200	ND
Dawson (1960), Maneveldt (2005), Maneveldt and Keats (2016)	Foslie (1900, 1909), Maneveldt (2005), Maneveldt and Keats (2016)	Foslie (1907, 1909), Maneveldt (2005), Richards et al. (2021)	Foslie (1907, 1909), Maneveldt (2005), Maneveldt and Keats (2016), Richards et al. (2021)	Maneveldt (2005), Maneveldt and Keats (2016), Taylor (1950), Woelkerling (1998)	Foslie (1907, 1909), Maneveldt (2005), Maneveldt and Keats (2016)

thick, firmly attached to the substratum, no free margins, lack of orbital ridges (Figure 7b). Surface texture smooth, matte, and granular due to presence of abundant, tightly packed, pustulate trichocyte fields (Figure 7c).

Vegetative anatomy: Thalli dorsiventrally organized, monomerous with medullary filaments predominately plumose (non-coaxial) in crustose areas (Figure 7d). Medullary cells square to rectangular, 6–12 μm long, 6–10 μm wide. Cortical cells square to rectangular, 4–15 μm long, 5–10 μm wide. Subepithallial initials

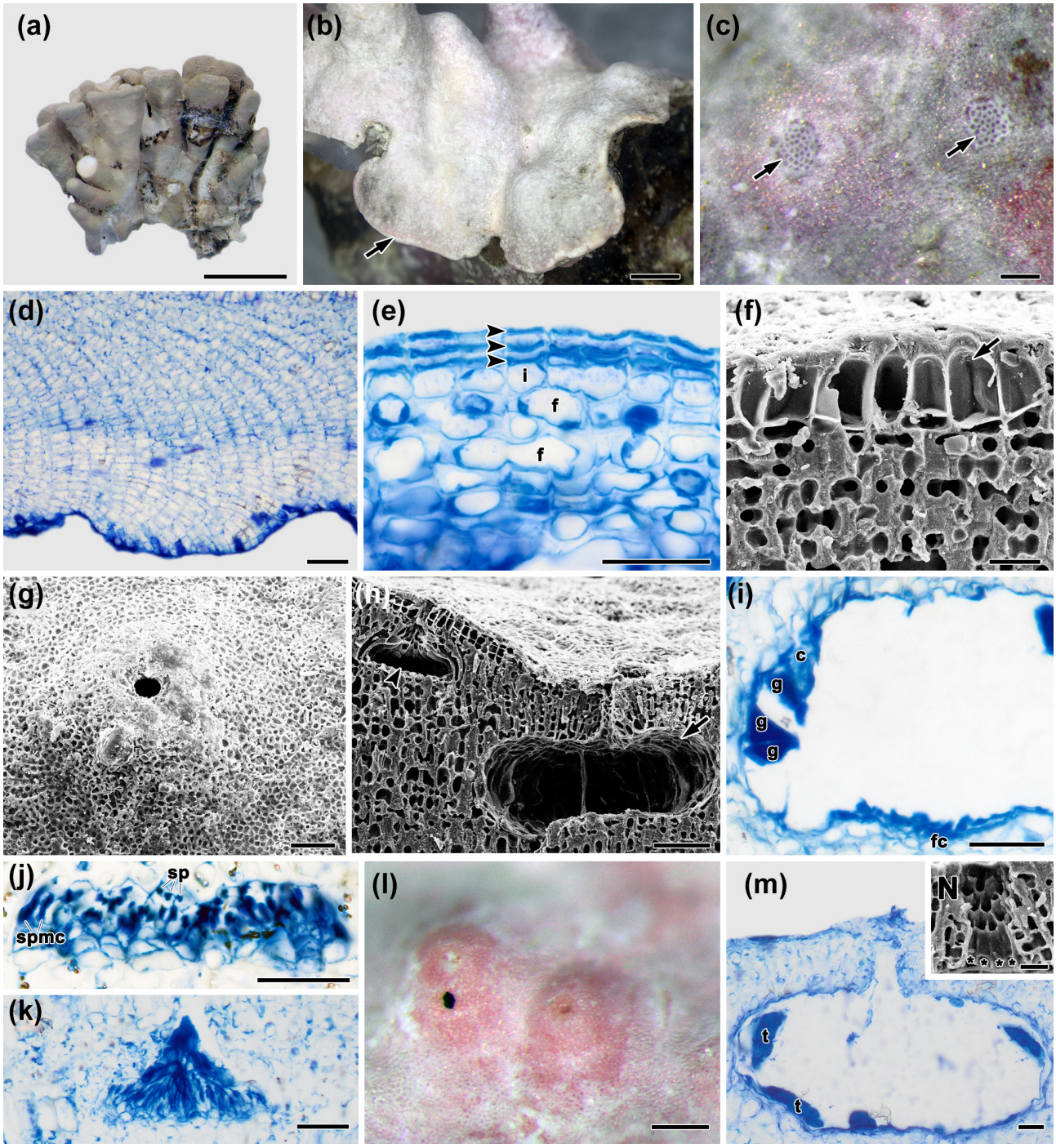

FIGURE 6 Vegetative and reproductive morpho-anatomy of *Porolithon lobulatum*. (a) Holotype specimen (BRI1040965). Scale bar = 1 cm. (b) Surface view showing free margin (arrow; DP-2450). Scale bar = 2 mm. (c) Surface view showing trichocyte fields (arrows; DP-2450). Scale bar = 200 μm. (d) Vertical section view of thallus showing monomerous construction and coaxial medullary filaments (DP-1110). Scale bar = 100 μm. (e) Vertical section view of outer thallus showing flattened epithallial cells (arrowheads), subepithallial initials (i) and cell fusions (f) between adjacent cortical filaments (DP-2625-1). Scale bar = 20 μm. (F) Vertical fracture through a trichocyte field (arrow; DP-1110). Note the absence of vegetative filaments between trichocyte megacells. Scale bar = 20 μm. (g) Magnified SEM surface view showing a raised female conceptacle (BRI1040965). Scale bar = 50 μm. (h) Vertical fracture through a monoecious thallus showing both female conceptacle (arrow) and a male conceptacle (arrowhead; BRI1040965). Scale bar = 50 μm. (i) Vertical section through a carposporangial conceptacle showing peripherally arranged gonimoblast filament (g) terminating in a carposporangium (c) from fusion cell (fc; DP-1268). Scale bar = 25 μm. (j) Vertical section through a spermatangial conceptacle showing spermatangial mother cells (spmc) and spermatangia (sp; DP-1268). Scale bar = 20 μm. (k) Vertical section through a spermatangial conceptacle showing simple spermatangial structures restricted to the conceptacle floor (DP-1268). Scale bar = 25 μm. (l) Surface view showing raised tetrasporangial conceptacles (DP-2625-1). Scale bar = 100 μm. (m) Vertical section through a tetrasporangial conceptacle showing elliptical-shaped chamber with tetrasporangia (DP-1110). Scale bar = 50 μm. (n) Vertical fracture through the edge of the pore canal of a tetrasporangial conceptacle showing the remains of the ring of enlarged cells (asterisks) located at the base of the pore canal (DP-1110). Scale bar = 25 μm.

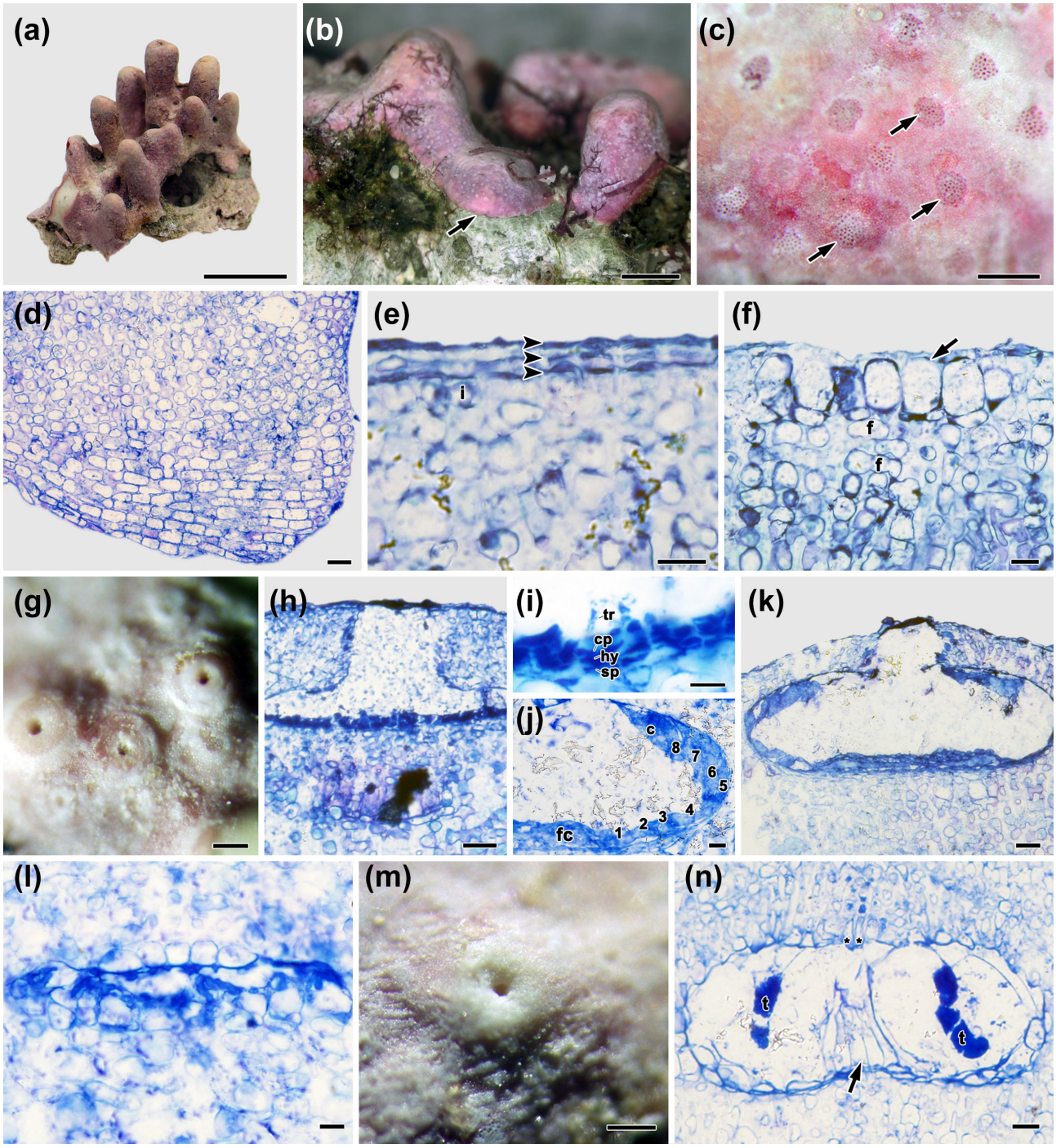

FIGURE 7 Vegetative and reproductive morpho-anatomy of *Porolithon parvulum*. (a) Holotype specimen (BRI1040960). Scale bar = 1 cm. (b) Surface view showing an adherent margin (arrow; DP-2248). Scale bar = 2 mm. (c) Surface view showing pustulate trichocyte fields (arrows; DP-2444). Scale bar = 200 μm. (d) Vertical section view of thallus showing monomerous construction (DP-2250). Scale bar = 20 μm. (e) Vertical section through the outer thallus showing a multi-layered epithallus comprising flattened cells (arrowheads), and subepithallial initials (i; DP-2250). Scale bar = 10 μm. (f) Vertical section through a trichocyte field (arrow) and cell fusions (f) between adjacent cortical filaments (DP-2250). Note the absence of vegetative filaments between trichocyte megacells. Scale bar = 10 μm. (g) Surface view of raised uniporate female conceptacles (DP-2249). Scale bar = 50 μm. (h) Vertical section through a carpogonial conceptacle showing elliptical-shaped chamber (DP-2249). Scale bar = 20 μm. (i) Magnified view of two-celled carpogonial branches composed of a hypogynous cell (hy) on a supporting cell (sp), and carpogonium (cp) with extended trichogyne (tr; DP-2257). Scale bar = 10 μm. (j) Magnified view of a eight-celled gonimoblast filament (numbers) terminating in a carposporangium (c) from a central fusion cell (fc; DP-2249). Scale bar = 10 μm. (k) Vertical section through a carposporangial conceptacle showing an elliptical-shaped chamber (DP-2249). Scale bar = 20 μm. (l) Vertical section through a buried male conceptacle showing simple spermatangial systems that are borne on the floor of the conceptacle chamber (DP-2249). Scale bar = 10 μm. (m) Surface view of a raised tetrasporangial conceptacle (BRI1040960). Scale bar = 100 μm. (n) Vertical section through a buried tetrasporangial conceptacle showing bean-shaped chamber with peripherally arranged tetrasporangia (t), central columella (arrow), and enlarged cells (asterisks) located at the base of the pore canal (DP-2250). Scale bar = 20 μm.

(intercalary meristematic cells) squarish with rounded corners, 3–9 μm in length, 4–12 μm in diameter (Figure 7e). Epithallus 1–3 layers of squat to elliptical cells, 1–5 μm long, 4–14 μm wide (Figure 7e). Cell fusions abundant; secondary pit connections not observed (Figure 7f). Trichocyte fields 69–148 μm in external diameter, 5–12 trichocytes grouped in vertical section, often overgrown and buried in thallus. Individual trichocytes rectangular to elongate, tightly packed and horizontally arranged without intervening cortical cells, 17–37 μm long, 6–18 μm wide (Figure 7f). Haustoria not observed.

Reproductive anatomy: Gametangial plants monoecious. Uniporate female conceptacles flush to raised to mound-shaped (Figure 7g), 117–225 μm in external diameter, 21–28 μm in external height above thallus surface. Two-celled carpogonial branches each borne on a supporting cell scattered across chamber floor (Figure 7h,i). Each carpogonial branch composed of hypogynous cell and carpogonium extended into a trichogyne (Figure 7i). After presumed karyogamy, carposporophytes developed in female conceptacles. Carposporangial conceptacle chambers elliptical, 242–310 μm in diameter, 76–100 μm in height, with roof 26–57 μm (6–10 cells; incl. epithallial cell) thick (Figure 7k). Conceptacle floor 11–14 cell layers below epithallus. Continuous central fusion cell narrow and thick (discoid), with gonimoblast filaments borne peripherally (Figure 7j,k). Gonimoblast filaments four to nine cells long including terminal carposporangium (Figure 7j). Uniporate male (spermatangial) conceptacles small, flush with surrounding thallus surface. Male conceptacle chambers elliptical, 67–78 μm in diameter, 9–13 μm in height, with roof 26–43 μm (6–11 cells; including epithallial cell) thick. Simple spermatangial systems borne only on floor of conceptacle chamber (Figure 7l). Both female and male conceptacles often buried.

Tetrasporangial conceptacles uniporate, 153–353 μm in external diameter, 31–115 μm in external height above surrounding thallus surface (Figure 7m). Conceptacle chambers elliptical to bean-shaped, 138–228 μm in diameter, 50–128 μm in height, with the roof 23–56 μm (5–10 cells; including epithallial cell) thick (Figure 7n). Conceptacle floor located 9–12 cells below epithallus. Pore canals 34–49 μm in length, 29–71 μm in diameter. Pore canal filaments orientated perpendicular, and not projecting into pore. Tetrasporangia zonately divided, 17–54 μm long, 6–19 μm wide (Figure 7n). A ring of enlarged cells lines the base of the pore canal (Figure 7n). Central columella observed (Figure 7n). Tetrasporangial conceptacles buried in thallus; infilled conceptacles not observed. Data on measured reproductive characters summarized in Table 1.

Porolithon pinnaculum S.Y.Jeong & G.Diaz-Pulido **sp. nov.** (Figures 8 and 9).

Holotype (designated here): BRI1040968, 27.ii.2022, growing attached to dead coral, 2.8 m deep, *leg*. Andrew Hoey; GenBank accessions: *rbc*L: OQ281547, *psb*A: OQ281500.

Isotypes: BRI1040971, BRI1040976, BRI1040977, BRI1040978 (*coll*. Andrew Hoey).

Type locality: Flora Reef, Coral Sea, Australia (16°45.313′ S, 147°43.911′ E).

Etymology: *pinnaculum* from the Latin *pinnaculum* meaning pinnacle and peak in reference to the thallus having pinnacle shaped protuberances.

Additional specimens examined: all confirmed by DNA sequencing (Table S1).

Habitat and geographic distribution: *Porolithon pinnaculum* occurs in shallow water coral reef environments, from reef crests to subtidal reef habitats to 9 m depth. It grows attached to the surface of coral skeletons and other carbonate substrates. Specimens confirmed by DNA sequencing were commonly found on several reefs and atolls in the Coral Sea (Diamond Islets, 17°31.2′ S, 150°17.3′ E; Flinders Reef, 17°36.016 S, 148°26.366′ E; Flora Reef, 16°45.313′ S, 147°43.911′ E; Herald Cay, 16°58.616′ S, 149°9.216′ E; Lihou Reef, 17°26.6′ S, 151°34.916′ E; and Marion Reef, 19°11.233′ S, 152°17.283′ E), Australia. This species is rare on the GBR and has only been found at Davies Reef (18°49.433′ S, 147°39.05′ E) in the central mid-shelf section of the GBR.

Description. Plants non-geniculate, columnar, massive, and mountain-like (Figure 8a,g), morphology variable with imbricate (overlapping) and artichoke-like habit (Figure 8h,i), bearing broad, individual to fused vertical protuberances (or columns). Protuberance apices variable from pointed to rounded to flattened and bifurcated, 11–97 mm long, 4–34 mm wide (Figure 9a). Living thalli greenish gray to orange to dark pink in color. Thallus margins firmly adherent or slightly loosely attached with corrugated-shaped edges depending on the substrate, but no free margins and lacking orbital ridges (Figure 9b). Surface texture smooth, matte, and granular due to the presence of abundant tightly packed, pustulate trichocyte fields (Figure 9c).

Vegetative anatomy: Thalli dorsiventrally organized, monomerous with medullary filaments predominately plumose (non-coaxial) in crustose areas. Cortical cells square to rectangular, 9–19 μm long, 5–13 μm wide. Subepithallial initials (intercalary meristematic cells) squarish with rounded corners, 5–10 μm in length, 5–10 μm in diameter (Figure 9d). Epithallus one to five layers of squat to elliptical cells, 2–5 μm long, 6–9 μm wide (Figure 9d). Cell fusions abundant (Figure 9e); secondary pit connections not observed. Trichocyte fields 93–173 μm in external diameter, 8–12 trichocytes grouped in vertical section (Figure 9e), often overgrown and buried. Individual trichocytes rectangular to elongate, tightly packed and horizontally arranged without

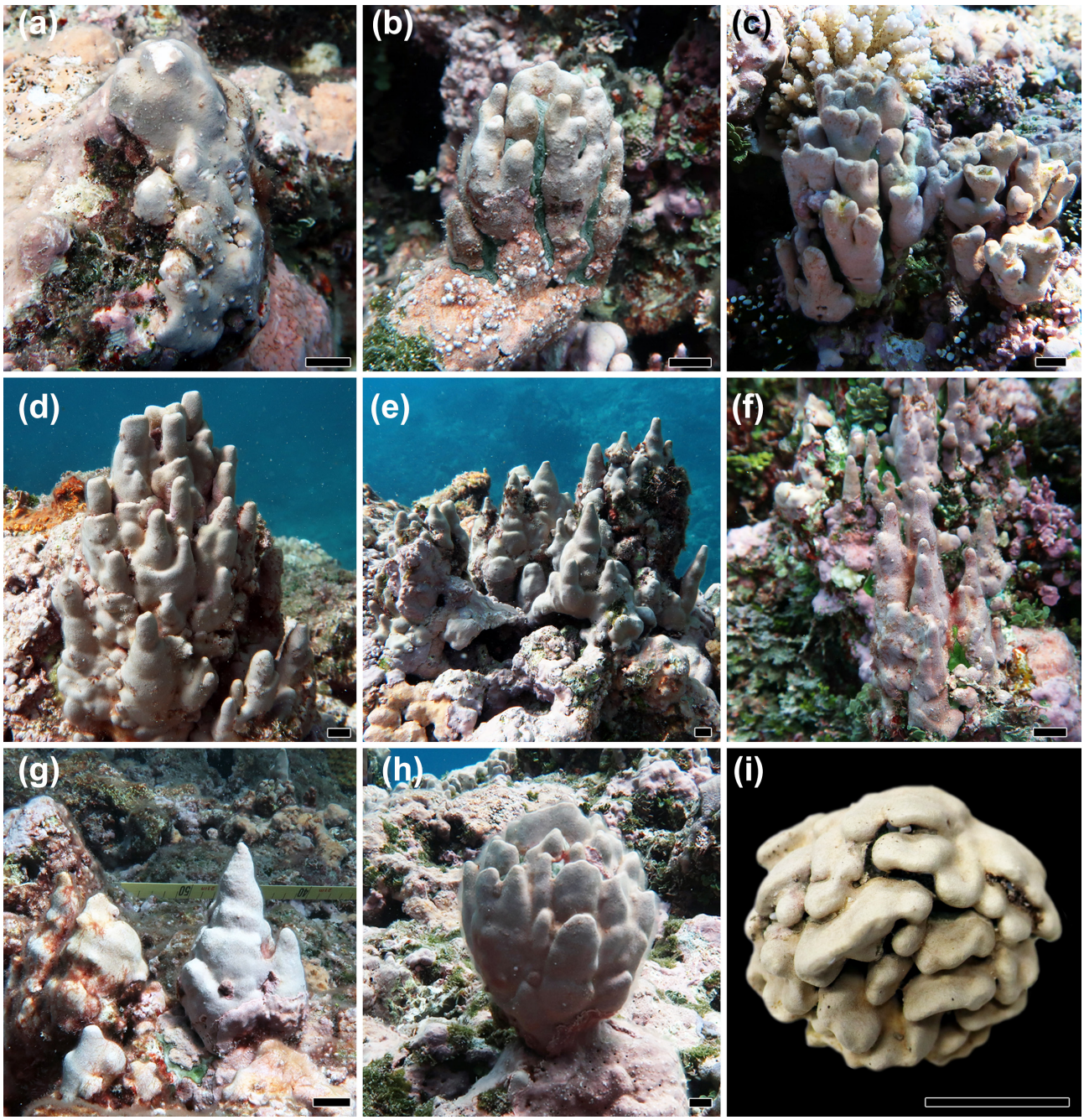

FIGURE 8 Field photos showing external morphological varieties of *Porolithon pinnaculum*. (a) Initial thallus growth stage with blunt protuberances (DP-2633-1). (b) Young thallus with short columnar branches (DP-2638-1). (c) Thallus with compressed and compact branches with concave apex (DP-2624). (d) Massive thallus bearing cylindrical branches with flattened or rounded apices (BRI1040968). (e) Massive thallus bearing cylindrical branches with pointed apex (BRI1040977). (f) Thallus bearing cylindrical and slender branches with pointed apices (DP-2635-1). (g) Thallus with pointed apex (BRI1040976). (h and i) Thallus bearing fused vertical "artichoke"-like protuberances (DP-2639-1). Scale bars = 1 cm.

intervening cortical cells, 17–30 μm long, 9–15 μm wide (Figure 9e). Haustoria not observed.

Reproductive anatomy: Gametangial plants not found. Tetrasporangial conceptacles uniporate, flush to slightly raised to mound-shaped above surrounding thallus surface, 139–201 μm in external diameter, 16–80 μm in external height above surrounding thallus surface (Figure 9f). Conceptacle chambers elliptical to bean-shaped, 160–203 μm in diameter, 75–155 μm in height, with roof 20–67 μm (4–8 cells; including epithallial cell) thick (Figure 9g). Conceptacle floor 11–16 cell layers below epithallus. Pore canals 30–63 μm in length, 24–47 μm in diameter. Pore canal filaments orientated perpendicular and not projecting into pore. Tetrasporangia zonately divided, 50–64 μm long, 8–37 μm wide (Figure 9g). Central columella not observed.

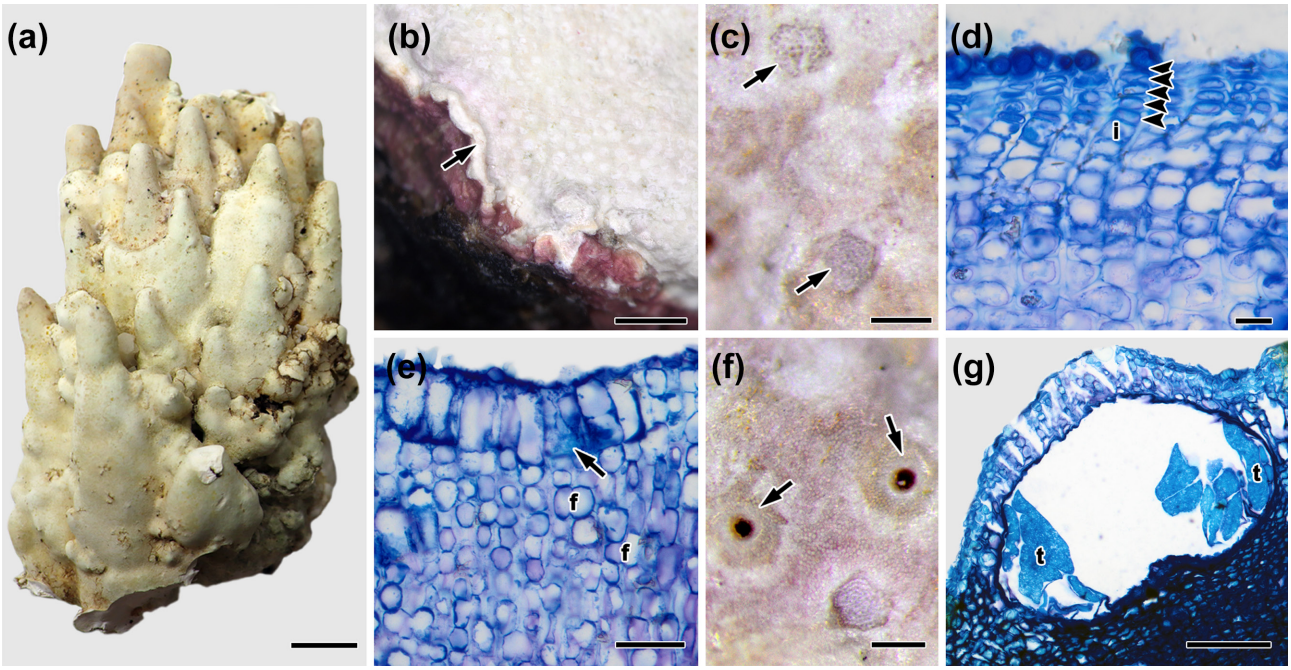

FIGURE 9 Vegetative and reproductive morpho-anatomy of *Porolithon pinnaculum*. (a) Holotype specimen (BRI1040968). Scale bar = 2 cm. (b) Surface view showing attached margin (arrow; DP-2629). Scale bar = 1 mm. (c) Surface view showing trichocyte fields (arrows; BRI1040971). Scale bar = 100 μm. (d) Vertical section view of outer thallus showing flattened epithallial cells (arrowheads) and subepithallial initials (i; DP-2615-1). Scale bar = 20 μm. (e) Vertical section through a trichocyte field (arrow) and cell fusions (f) between adjacent cortical filaments (BRI1040971). Note the absence of vegetative filaments between trichocyte megacells. Scale bar = 25 μm. (f) Surface view showing raised tetrasporangial conceptacles (arrows; BRI1040971). Scale bar = 100 μm. (g) Vertical section through a tetrasporangial conceptacle showing elliptical-shaped chamber with tetrasporangia (t; DP-2462). Scale bar = 50 μm.

Tetrasporangial conceptacles buried in thallus; infilled conceptacles not observed. Data on measured reproductive characters summarized in Table 1.

DISCUSSION

Phylogenetic analyses of *rbc*L and *psb*A sequences and morpho-anatomical observations show that *Porolithon* specimens with branching morphology resembling *P. castellum*, *P. craspedium*, and *P. gardineri* collected from the Australian GBR, Coral Sea, and Lord Howe Island represent previously undescribed species. We therefore proposed four species new to science: *P. howensis*, *P. lobulatum*, *P. parvulum*, and *P. pinnaculum*. The phylogenetic trees of *rbc*L and *psb*A gene sequences confirm these species belong to *Porolithon*, and they occur in strongly supported clades. Morpho-anatomical documentation of the new species supports the character of having horizontal fields of trichocytes without intervening vegetative cells (Figures 5c, 6f 7f and 9e) as diagnostic for *Porolithon* (Foslie, 1909; Kato et al., 2011; Maneveldt & Keats, 2014, 2016; Richards et al., 2021). The four new species show significant sequence divergences (0.7%–9.1% in *rbc*L; 3.2%–6.1% in *psb*A) from other closely related branching *Porolithon* species, providing support for the new species herein proposed. Phylogenetic analyses of the *rbc*L gene sequences of type specimens further reveal that *P. castellum* is not conspecific with *P. craspedium*, as suggested by Maneveldt and Keats (2016) solely based on morpho-anatomy. Further, *P. craspedium*, which had been considered to belong in *Lithophyllum* (Adey & Lebednik, 1967; Foslie, 1900; Tittley et al., 1984) or *Hydrolithon* (Penrose & Woelkerling, 1992; Silva et al., 1996) or *Porolithon* (Adey, 1970; Maneveldt & Keats, 2016), is herein confirmed as indeed belonging in a clade with the generitype of *Porolithon*, *P. onkodes* (as suggested by Bittner et al., 2011, p. 710). These results emphasize the importance of sequencing both new collections and type material to distinguish species, to correctly apply names, and to document the diversity more accurately in crustose coralline algae.

Comparison among *P. pinnaculum*, *P. howensis*, and other massive species

Porolithon pinnaculum is morphologically very similar to *P. castellum* (type locality: Isla del Caño, Costa Rica, Eastern Pacific), *P. craspedium* (type locality: Onotoa, Kiribati, Central Pacific), and, to some extent, *P. howensis*, as they all share a massive, columnar

thallus with broad individual to fused vertical columns. However, *P. pinnaculum* differs from *P. castellum* and *P. craspedium* in having attached margins, whereas *P. castellum* and *P. craspedium* form free margins that are entire to lobed (Maneveldt & Keats, 2016; Table 1). Importantly, *P. pinnaculum* has considerable sequence divergence in its *rbc*L gene with respect to *P. castellum* (7.4%–8.3%) and *P. craspedium* (5.1%–5.9%), indicating that these are distinct species. The *rbc*L gene sequence divergence between *P. howensis* and the isotype sequence of *P. castellum* is only 0.7% (1 bp difference among 136 bp), which is a relatively low value considering the large geographic distance separating the two type localities (>13,185 km). However, values of sequence divergence of >0.5%–0.8% in the *rbc*L gene have also been used in other corallines to separate species (e.g., *Calliarthron*, Gabrielson et al., 2011; *Crusticorallina*, Hind et al., 2016; *Porolithon*, Gabrielson et al., 2018). Further, *P. howensis* and *P. castellum* vary in their external morphology, with the latter having narrow, elongated branches while *P. howensis* has more robust, thicker, but shorter protuberances.

Comparison among *P. lobulatum*, *P. parvulum*, and *P. gardineri*

The other two species with branched morphology described here, *Porolithon lobulatum* and *P. parvulum*, are less massive than *P. pinnaculum* and resemble *P. gardineri* in forming smooth to lumpy to fruticose thalli bearing shallow terete protuberances that grow individually or fused (Maneveldt & Keats, 2016). Some specimens of *P. lobulatum* and *P. parvulum* may also exhibit columnar specimens (not truly terete morphologies) but are certainly less robust than *P. pinnaculum* and *P. howensis*. However, the two new species are distinguished from *P. gardineri* based on a combination of margin shape and thallus construction in the crustose portion. *Porolithon parvulum* differs from *P. gardineri* in having attached margins, whereas *P. lobulatum* is distinguished from *P. gardineri* and all other currently described branched *Porolithon* species by having coaxial thallus construction in the crustose portion (Figure 6d; Table 1). In addition to the morpho-anatomical differences presented here, genetic discontinuities among the species were also clear. The pairwise comparisons between *P. gardineri* and the two newly described species, *P. lobulatum* and *P. parvulum*, show gene sequence divergence values of 8.4%–9.9% in *rbc*L, providing strong support to recognize the two new species. *Porolithon marshallense* W.R. Taylor, another species with a branching morphology (Table 1), can be distinguished from *P. lobulatum* and *P. parvulum* by its general habit and branching pattern, being cushion-shaped to hemispherical with erect-radiating branches (Maneveldt & Keats, 2016; Taylor, 1950). None of the new species proposed here exhibit this morphology; however, DNA sequences of the type of *P. marshallense* are not available, and its definitive relationship with the new species is uncertain.

Within the *Porolithon lobulatum* clade there are two subclades with strong support (96%/1 in *rbc*L, 100%/1 in *psb*A), one comprising specimens from oceanic reefs of the Coral Sea Marine Park (Diamond Islets, Lihou and Marion Reefs) and the other including specimens from the GBR (northern, central, and southern sections), distributions that suggest the existence of two different populations (or species) within the *P. lobulatum* lineage. Intraspecific differences in our *P. lobulatum* sequences in the *rbc*L and *psb*A genes were 0.7%–2.0% and 0.5%–0.7%, respectively, and this may support the hypothesis of recent divergence between oceanic Coral Sea and GBR populations. As a comparison, cryptic species recognized in other genera of Corallinales differed by >0.7%–0.8% in the *psb*A gene and >0.5%–0.8% in the *rbc*L gene (Gabrielson et al., 2011, 2018; Hind et al., 2016; Pezzolesi et al., 2019). Despite the genetic differences, we were not able to find any morpho-anatomical discontinuities to separate the Coral Sea from the GBR populations of *P. lobulatum* based on material currently available. These populations may represent cryptic species (i.e., taxa that are morphologically indistinguishable but are on different evolutionary trajectories; but see Struck et al., 2018 for debate on the use of this term). Evolution is an ongoing process, and the difficulty in recognizing populations/species is to be expected. We acknowledge that although the separation between the species *P. castellum* and *P. howensis* was based on a divergence value of 0.7% for *rbc*L, the geographic difference and distance between their type localities (>13,185 km) is an argument for their separation. The pairwise divergence for *rbc*L between the two sub-clades of *P. lobulatum* was 0.7%–2.0%, higher than that between *P. castellum* and *P. howensis*, but the geographic distance is only 350 km, providing limited argument for the separation of species within the *P. lobulatum* sub-clades. Further, given the lack of morphological disparity between the two subclades, we prefer to wait until further evidence is obtained (e.g., physiological, ecological, etc.) before proposing a new species. The *psb*A sequences from *P. lobulatum* corresponding to the Coral Sea clade were very similar (0.2%–0.7%) to that obtained from an unidentified *Porolithon* taxon collected in the Gambier Islands, French Polynesia, Central Pacific by Caragnano et al. (2018; MG851064.1, as *Porolithon* sp. NOU 087027). The Caragnano et al. (2018) material would thus appear to be *P. lobulatum*, and this would considerably extend the distribution range of this species to >6500 km. It is also worth noting that the French Polynesian sequence clustered with specimens from the oceanic reefs of the Coral Sea, not the GBR subclade, supporting the occurrence of two distinct populations

(or species) separated geographically. Further DNA sequencing and phylogenetic research is needed to determine if the GBR clade of *P. lobulatum* is endemic to the GBR region.

Porolithon castellum and *P. craspedium* are different species

The phylogenetic analyses also demonstrate that two species that had been proposed as conspecifics due to their similar morphology, *Porolithon castellum* and *P. craspedium*, are in fact different taxa. Maneveldt and Keats (2016) reviewed the taxonomy of branched *Porolithon* species based solely on morpho-anatomical examination of type material and comparisons with other closely related species. They suggested that *P. castellum* may be conspecific with *P. craspedium* because they share both a massive and mountain-like morphology and a small-sized ring of enlarged cells that lines the base of the pore canal in tetrasporangial conceptacles. However, based on 118 bp *rbc*L gene sequences from the isotype specimen of *P. castellum* and holotype specimen of *P. craspedium*, both are distinct species with a sequence divergence value of 8.5%. DNA sequences from both *P. castellum* and *P. craspedium* indicate that they are known only from their type localities in Costa Rica and Onotoa, Kiribati, respectively. All other reports of *P. craspedium* from Africa (Silva et al., 1996; Vieira et al., 2021), Indian Ocean Islands (Silva et al., 1996), Korea (Lee, 2008), Pacific Islands (Eniwetok Atoll: Dawson, 1957; Guam: Johnson, 1964; Littler & Littler, 2003; Bikini Atoll: Johnson, 1954), South America (Juan Fernandez Islands: Levring, 1943), and South-west Asia (Silva et al., 1996) need to be confirmed by DNA sequencing to determine if this is indeed a widely distributed species. Based on the DNA sequencing results of all other *Porolithon* species to date, a widespread distribution of *P. craspedium* seems unlikely.

Geographic distribution of branching *Porolithon*

Mature specimens of *Porolithon pinnaculum* that have been confirmed with DNA sequencing are currently only known from oceanic coral reefs and atolls of the Queensland Plateau (350–400 km offshore from the Australian mainland) in the Coral Sea Marine Park. Except for the locality of the sequenced type specimen, all other reports of *P. craspedium* across the entire tropical Pacific Ocean, from the Juan Fernandez archipelago off the coast of Chile in the eastern Pacific to Guam in the western Pacific (Johnson, 1964), are based on morpho-anatomy, and their true identities need to be confirmed with molecular methods. It is also likely that specimens of *P. pinnaculum* are passing under *P. craspedium* given the morphological similarity between the two species (Table 1). Without DNA sequencing of these specimens, however, it is difficult to know the true geographic distribution range of either *P. pinnaculum* or *P. craspedium*. A unique, small-size individual of *P. pinnaculum* (DP-2462), confirmed by *rbc*L gene sequencing, was collected from Davies Reef in the central GBR, around 350 km from the closest reef in the Coral Sea where *P. pinnaculum* commonly occurs. Extensive surveys of CCA in reefs along the GBR have failed to record specimens with massive and mound-like morphologies, such as *P. pinnaculum* or *P. craspedium* (e.g., Dean et al., 2015; G. Diaz-Pulido, personal observation; Ringeltaube & Harvey, 2000), nor have they been recorded in the fossil record of the GBR (Braga & Aguirre, 2004). The only species with large branches and a columnar appearance currently present along the GBR is *Adeylithon bosencei* (Peña et al., 2018), but this species is anatomically very different to any *Porolithon* species because it lacks trichocytes arranged in tightly packed horizontal fields without interspersed vegetative filaments (*A. bosencei* trichocyte fields are loosely packed) and because it has the outline of cell filaments entirely lost due to pervasive and extensive cell fusions. The absence of massive, columnar forms of *Porolithon*, such as *P. craspedium*, *P. howensis*, and *P. pinnaculum* from the GBR, is intriguing, particularly since the types of environments in which *P. craspedium* and *P. pinnaculum* grow in the central Pacific and oceanic reefs of the Coral Sea, are also present along the GBR, such as windward reef spurs and buttresses and other highly exposed habitats with good water circulation (Johnson, 1964; Littler & Littler, 2003). These massive columnar forms of *Porolithon* are typical of oceanic coral reefs, distant from significant continental influence. It is therefore plausible that the relative proximity of GBR reefs to terrestrial runoff (particularly during the early development of the GBR in the medium to late Pleistocene) limited the establishment of such massive columnar forms of *Porolithon* species in this region. Future collections from the outer reefs of the GBR need to be sequenced to confirm the presence of these massive columnar forms of *Porolithon*.

Porolithon howensis is known only from the two localities from which specimens were collected: Lord Howe Island (New South Wales) and Tideway Reef (central GBR, Queensland). Specimens collected from Lord Howe Island grow on reef front terraces with high wave energy are well developed with thick protuberances (Figure 4a). It is common, but not locally abundant (although accurate estimates of its abundance would require material to be confirmed by DNA sequencing), and it seems to occur in areas of high grazing by urchins. The small crust from the GBR

(Tideway Reef) had incipient protuberances and may not be a fully developed specimen (Figure 4b), and it resembles specimens of the "chalky" color morph of smooth (unbranched) *Porolithon* from the GBR. A parallel study currently underway, examining the smooth (unbranched) forms of *Porolithon*, will examine how distinct this comparatively smooth specimen of *P. howensis* is from other smooth forms from the GBR. As mentioned earlier, the *rbc*L gene sequence of *P. howensis* differs only in 1 bp from that of the type of *P. castellum*; however, given the geographic separation (>13,185 km) and distinct external morphology, these specimens are considered different species. Therefore, until further evidence becomes available, *P. howensis* is endemic from Lord Howe Island and the GBR.

Porolithon parvulum is restricted to the central and southern sections of the GBR. Genetically identified specimens of *P. parvulum* have only been confirmed from shallow, well-exposed coral reef environments of outer and mid-shelf reefs in the central GBR and Heron Island, the latter a platform reef in the southern GBR. It is unclear whether the records of *P. gardineri* from Dean et al. (2015), which were identified based on morphological characters only, refer to *P. lobulatum*, *P. parvulum*, or a combination of both. The type locality of *P. gardineri* is Coevity Reef, Chagos Archipelago in the western Indian Ocean, a locality 10,100 km from the GBR. Given the high rates of speciation in *Porolithon* (Gabrielson et al., 2018), it is unlikely that *P. gardineri* occurs in the GBR. Although *P.* "*gardineri*" has been recorded across the Pacific Ocean based on morpho-anatomy (e.g., Hawaii: Adey et al., 1982; Magruder & Hunt, 1979; Indonesia: Verheij, 1994; Wider Pacific: Littler & Littler, 2003; Maneveldt & Keats, 2016; Guam: Gordon et al., 1976, Micronesia: Lobban & Tsuda, 2003; Easter Island: Santelices & Abbott, 1987), large variability in branching patterns and size of branches/protuberances exists. Thus, it is likely that the *P.* "*gardineri*" group is also composed of several species. Further research, using DNA sequencing evidence, will help to clarify the distributions of *P. parvulum*, *P. gardineri*, and other columnar taxa.

Porolithon lobulatum has a much wider distribution than *P. parvulum*, with DNA sequencing confirmed records spanning 1190 km from the northern, central, and southern sections of the GBR and several oceanic reefs from the Queensland Plateau in the Coral Sea. No records exist from other localities not sampled in this study. We found no clear genetic or morpho-anatomical distinction between populations from the different sections of GBR, but the GBR populations are genetically distinct from those of the Coral Sea (as discussed above; Figures 2 and 3). It can therefore be hypothesized that the population of *P. lobulatum* from the GBR is in an early process of speciation (discussed below).

The four new species of *Porolithon* with a branching morphology add to the existing seven species of branching *Porolithon* that have been described in the literature: *P. aequinoctiale* (type locality: São Tomé and Príncipe); *P. castellum*, *P. coarctatum* (type locality: Cocos-Keeling Islands); *P. craspedium*, *P. gardineri*, *P. marshallense* (type locality: Rongelap Atoll, Marshall Islands); and *P. praetextatum* (type locality: Easter Island; Table 1). Two species, *P. coarctatum* and *P. gardineri* are distributed in the eastern and western Indian Ocean, respectively (based on DNA sequence), while *P. castellum* and *P. praetextatum* (not confirmed with DNA) are only known from their type localities in the Eastern Tropical Pacific (America). The only species with branching morphology known from the Atlantic, *P. aequinoctiale*, is from the west coast of Africa, off Equatorial Guinea (Foslie, 1909). As a morphologically defined group these *Porolithon* species have a pantropical distribution.

Potential origin of the species

Porolithon has a relatively recent origin among the Corallinophycidae, with records of smooth specimens dating back to the period between late Oligocene and middle Miocene, from coastal reefs from Borneo, Indonesia (Rösler et al., 2015, 2017). Fossils of branching *Porolithon* have been found in rocks of a much more recent origin; for example, specimens called *P. craspedium* have been recovered from the Pliocene and Pleistocene from Guam (Johnson, 1964), the Pleistocene from Bikini Atoll (Johnson, 1954), and Funafuti Atoll (Johnson, 1961). According to Johnson (1961), *Porolithon* did not become abundant in oceanic coral reefs of the Pacific until the middle of the Pleistocene. There are records of specimens called *P. gardineri* found in drill cores of the GBR dating from the Pleistocene (specifically ca. ~130–116 ka; Dechnik et al., 2017), although smooth specimens of the *Porolithon* "*onkodes*" complex are much more abundant than those called *P. gardineri* in those cores (Braga & Aguirre, 2004; Dechnik et al., 2017). There are no fossil records of massive, columnar species of *Porolithon* (e.g., *P. craspedium* or *P. pinnaculum*) from the GBR (Braga & Aguirre, 2004; Dechnik et al., 2017) nor from oceanic reefs from the Queensland Plateau (Martín & Braga, 1993). Despite the existence of fossils of fruticose *Porolithon* ("*gardineri*") recovered from drill holes in the GBR (Dechnik et al., 2017), it is difficult to determine if those specimens correspond to *P. parvulum* or *P. lobulatum*. Given the complex geological history of the carbonate platforms and coral reefs from northern Australia and the Coral Sea (Ceccarelli et al., 2013; Davies et al., 1989) and

recurrent glacio-eustatic oscillations (some up to 120 m during the Pleistocene in the region, Braga & Aguirre, 2004), it is difficult to elucidate the processes of speciation that lead to the origin of the new species described here. During low sea-level periods the GBR and Coral Sea reefs were emergent, and reefs were exposed to erosion and increased terrigenous inputs, perhaps restricting species with an oceanic water requirement, while higher sea levels promoted active carbonate deposition, perhaps facilitating not only species dispersal and colonization but also replacement of shallow-water coralline algal florae (e.g., dominated by *Porolithon* spp.) by deep water species (Braga & Aguirre, 2004). Sea-level oscillations may have isolated some populations geographically (allopatric speciation) or may have promoted founder effect speciation during highstands. The complex geological history and other evolutionary processes (Gabrielson et al., 2018) may have contributed to the high diversification of coralline algae in this region (Bittner et al., 2011; Ceccarelli et al., 2013).

Concluding remarks

Finally, given the ecological significance of *Porolithon* species that grow abundantly along shallow reef margins and that cement reef frameworks (e.g., Adey, 1978a; Johnson, 1961; Littler & Littler, 2013) and induce settlement of coral larvae (Diaz-Pulido et al., 2010; Heyward & Negri, 1999), it is important that the taxonomy of this genus is clarified. This is particularly important when considering the several synonymies previously suggested. Furthermore, species of *Porolithon* are one of the most sensitive to the impacts of ocean acidification (Anthony et al., 2008; Bergstrom et al., 2023; Diaz-Pulido et al., 2012; Johnson & Carpenter, 2012; Page et al., 2022). An accurate delimitation of the species and a better understanding of their diversity and phylogenetic relationships will help elucidate their biogeographical and ecological roles, and their vulnerabilities to environmental change and potential to adapt to a rapidly changing climate.

AUTHOR CONTRIBUTIONS

So Young Jeong: Conceptualization (lead); data curation (lead); formal analysis (lead); investigation (lead); methodology (lead); resources (equal); software (lead); visualization (lead); writing – original draft (equal); writing – review and editing (equal). **Paul W. Gabrielson:** Data curation (equal); resources (equal); writing – review and editing (equal). **Jeffery R. Hughey:** Formal analysis (equal); methodology (equal); writing – review and editing (equal). **Andrew S. Hoey:** Resources (equal); writing – review and editing (equal). **Tae Oh Cho:** Resources (equal); writing – review and editing (equal). **Muhammad A. Abdul Wahab:** Resources (equal); writing – review and editing (equal). **Guillermo Diaz-Pulido:** Conceptualization (equal); data curation (equal); funding acquisition (lead); investigation (equal); project administration (lead); resources (equal); supervision (equal); writing – original draft (equal); writing – review and editing (equal).

ACKNOWLEDGMENTS

We would like to thank Dr Christian Hassel and Tommy Prestø (TRH) and UC for generous loans of collections from the Foslie herbarium and specimen of Dawson, and the crew of the MV Iron Joy for logistic support in the Coral Sea. Dr Alexandra Ordonez and Tessa Page helped with collections, and Dr C. Arango with analyses and discussions. Open access publishing facilitated by Griffith University, as part of the Wiley - Griffith University agreement via the Council of Australian University Librarians.

FUNDING INFORMATION

SYJ and GD-P are deeply thankful to the Department of the Environment and Energy of the Australian Government, through the Australian Biological Resources Study (ABRS), National Taxonomy Research Grant Program (NTRGP, RG19-35). Grants from the Great Barrier Reef Foundation (GBRF), the Australian Research Council (ARC, DP160103071) have also supported this research. Thanks also for the support from the Reef Restoration and Adaptation Program (RRAP) and the Australian Institute of Marine Science (AIMS) and the Director of National Parks (DNP). DNA extraction and sequencing performed by JRH were funded by the generous support from a private family trust (PWG). This research was also supported by the Basic Science Research Program through the National Research Foundation of Korea (NRF) funded by the Ministry of Education (2021R1I1A2059577), the Ministry of Ocean and Fisheries (Marine Biotics Project, 20210469), and National Marine Biodiversity Institute of Korea (the management of Marine Fishery Bio-resources Center 2023) to TOC.

CONFLICT OF INTEREST STATEMENT

The authors declare no conflict of interest.

ORCID

So Young Jeong https://orcid.org/0000-0002-6803-3875
Paul W. Gabrielson https://orcid.org/0000-0001-9416-1187
Jeffery R. Hughey https://orcid.org/0000-0003-4053-9150
Andrew S. Hoey https://orcid.org/0000-0002-4261-5594
Tae Oh Cho https://orcid.org/0000-0003-4250-818X
Muhammad A. Abdul Wahab https://orcid.org/0000-0003-4088-9652

Guillermo Diaz-Pulido https://orcid.org/0000-0002-0901-3727

REFERENCES

Adey, W. H. (1970). A revision of the Foslie crustose coralline herbarium. *Det Kongelige Norske Videnskabers Selskabs Skrifter [the Writings of the Royal Norwegian Society of Sciences]*, *1*, 1–46.

Adey, W. H. (1978a). Algal ridges of the Caribbean Sea and West Indies. *Phycologia*, *17*, 361–367.

Adey, W. H. (1978b). Coral reef morphogenesis: A multidimensional model. *Science*, *202*, 4370–4837.

Adey, W. H. (1998). Coral reefs: Algal structured and mediated ecosystems in shallow, turbulent, alkaline waters. *Journal of Phycology*, *34*, 393–406.

Adey, W. H., & Adey, P. J. (1973). Studies on the biosystematics and ecology of the epilithic crustose Corallinaceae of the British Isles. *British Phycological Journal*, *8*, 343–407.

Adey, W. H., & Lebednik, P. (1967). *Catalog of the Foslie Herbarium*. Del Kongelige norske Videnskabers Selskab Museet [Royal Norwegian Society of Sciences Museum].

Adey, W. H., Townsend, R. A., & Boykins, W. T. (1982). The crustose coralline algae (Rhodophyta: Corallinaceae) of the Hawaiian islands. *Smithson Contribributions in Marine Science*, *15*, 1–74.

Anthony, K. R. N., Kline, D. I., Diaz-Pulido, G., Dove, S., & Hoegh-Guldberg, O. (2008). Ocean acidification causes bleaching and productivity loss in coral reef builders. *Proceedings of the National Academy of Sciences*, *105*, 17442–17446.

Bergstrom, E., Lahnstein, J., Collins, H., Page, T., Bulone, V., & Diaz-Pulido, G. (2023). Cell wall organic matrix composition and biomineralization across reef-building coralline algae under global change. *Journal of Phycology*, *59*, 111–125.

Birkeland, C., Green, A., Lawrence, A., Coward, G., Vaeoso, M., & Fenner, D. (2021). Different resiliencies in coral communities over ecological and geological time scales in American Samoa. *Marine Ecology Progress Series*, *673*, 55–68.

Bittner, L., Payri, C. E., Maneveldt, G. W., Couloux, A., Cruaud, C., de Reviers, B., & Le Gall, L. (2011). Evolutionary history of the Corallinales (Corallinophycidae, Rhodophyta) inferred from nuclear, plastidial and mitochondrial genomes. *Molecular Phylogenetics and Evolution*, *61*, 697–713.

Bjork, M., Mohammad, S. M., Bjorklund, M., & Semesi, A. (1995). Coralline algae, important coral reef builders threatened by pollution. *Ambio*, *24*, 502–505.

Bosence, D. W. J. (1983). Coralline algal reef frameworks. *Journal of the Geographical Society of London*, *140*, 365–376.

Braga, J. C., & Aguirre, J. (2004). Coralline algae indicate Pleistocene evolution from deep, open platform to outer barrier reef environments in the northern Great Barrier Reef margin. *Coral Reefs*, *23*, 547–558.

Caragnano, A., Foetisch, A., Maneveldt, G., Millet, L., Liu, L. C., Lin, S. M., Rodondi, G., & Payri, C. E. (2018). Revision of Corallinaceae (Corallinales, Rhodophyta): Recognizing *Dawsoniolithon*, gen. Nov., *Parvicellularium* gen. Nov. and Chamberlainioideae subfam. Nov. containing, *Chamberlainium* gen. Nov. and *Pneophyllum*. *Journal of Phycology*, *54*, 391–409.

Ceccarelli, D. M., McKinnon, A. D., Andrefouet, S., Allain, V., Young, J., Gledhill, D. C., Flynn, A., Bax, N. J., Beaman, R., Borsa, P., Brinkman, R., Bustamante, R. H., Campbell, R., Cappo, M., Cravatte, S., D'Agata, S., Dichmont, C. M., Dunstan, P. K., Dupouy, C., … Richardson, A. J. (2013). The Coral Sea: Physical environment, ecosystem status and biodiversity assets. *Advances in Marine Biology*, *66*, 213–290.

Chamberlain, Y. M. (1990). The genus *Leptophytum* (Rhodophyta, Corallinaceae) in the British Isles with descriptions of *Leptophytum bornetii*, *L. elatum* sp. nov. and *L. laeve*. *British Phycological Journal*, *25*, 179–199.

Daume, S., Brand-Gardner, S., & Woelkerling, W. J. (1999). Settlement of abalone larvae (*Haliotis laevigata* Donovan) in response to non-geniculate coralline red algae (Corallinales, Rhodophyta). *Journal of Experimental Marine Biology and Ecology*, *234*, 125–143.

Davies, P. J., Symonds, P. A., Feary, D. A., & Pigram, C. J. (1989). The evolution of the carbonate platforms of Northeast Australia. In P. D. Crevello (Ed.), *Controls on carbonate platform and basin development* (pp. 233–258). Society for Sedimentary Geology.

Dawson, E. Y. (1957). An annotated list of marine algae from Eniwetok atoll, Marshall Islands. *Pacific Science*, *11*, 92–132.

Dawson, E. Y. (1960). Marine red algae of Pacific Mexico. part 3. Cryptonemiales, Corallinaceae Subf. Melobesioideae. *Pacific Science*, *2*, 3–125.

Dean, A. J., Steneck, R. S., Tager, D., & Pandolfi, J. M. (2015). Distribution, abundance and diversity of crustose coralline algae on the great barrier reef. *Coral Reefs*, *34*, 581–594.

Dechnik, B., Webster, J. M., Webb, G. E., Nothdurft, L., Dutton, A., Braga, J. C., Zhao, J., Duce, S., & Sadler, J. (2017). The evolution of the Great Barrier Reef during the last interglacial period. *Global and Planetary Change*, *149*, 53–71.

Diaz-Pulido, G., Anthony, K. R. N., Kline, D. I., Dove, S., & Hoegh-Guldberg, O. (2012). Interactions between ocean acidification and warming on the mortality and dissolution of coralline algae. *Journal of Phycology*, *48*, 32–39.

Diaz-Pulido, G., Harii, S., McCook, L. J., & Hoegh-Guldberg, O. (2010). The impact of benthic algae on the settlement of a reef-building coral. *Coral Reefs*, *29*, 203–208.

Diaz-Pulido, G., McCook, L. J., Larkum, A. W. D., Lotze, H. K., Raven, J. A., Schaffelke, B., Smith, J. E., & Steneck, R. S. (2007). Vulnerability of macroalgae of the Great Barrier Reef to climate change. In J. E. Johnson & P. A. Marshall (Eds.), *Climate change and the Great Barrier Reef* (pp. 153–192). Great Barrier Reef Marine Park Authority & Australian Greenhouse Office.

Diaz-Pulido, G., Nash, M. C., Anthony, K. R. N., Bender, D., Opdyke, B. N., Reyes-Nivia, M., & Troitzsch, U. (2014). Greenhouse conditions induce mineralogical changes and dolomite accumulation in coralline algae on tropical reefs. *Nature Communications*, *5*, 3310.

Doropoulos, C., Roff, G., Bozec, Y. M., Zupan, M., Werminghausen, J., & Mumby, P. J. (2016). Characterizing the ecological trade-offs throughout the early ontogeny of coral recruitment. *Ecological Monographs*, *86*, 20–44.

Foslie, M. (1900). New or critical calcareous algae. *Det Kongelige Norske Videnskabers Selskabs Skrifter [the Writings of the Royal Norwegian Society of Sciences]*, *5*, 1–34.

Foslie, M. (1907). Algologiske notiser [Algological notices] III. *Det Kongelige Norske Videnskabers Selskabs Skrifter [the Writings of the Royal Norwegian Society of Sciences]*, *8*, 1–34.

Foslie, M. (1909). Algologiske notiser [Algological notices] VI. *Det Kongelige Norske Videnskabers Selskabs Skrifter [the Writings of the Royal Norwegian Society of Sciences]*, *2*, 1–9.

Freshwater, D. W., & Rueness, J. (1994). Phylogenetic relationships of some European *Gelidium* (Gelidiales, Rhodophyta) species, based on *rbc*L nucleotide sequence analysis. *Phycologia*, *33*, 187–194.

Gabrielson, P. W., Hughey, J. R., & Diaz-Pulido, G. (2018). Genomics reveals abundant speciation in the coral reef building alga *Porolithon onkodes* (Corallinales, Rhodophyta). *Journal of Phycology*, *54*, 429–434.

Gabrielson, P. W., Miller, K. A., & Martone, P. T. (2011). Morphometric and molecular analyses confirm two distinct species of

Calliarthron (Corallinales, Rhodophyta), a genus endemic to the Northeast Pacific. *Phycologia*, *50*, 298–316.
Gordon, G. D., Masaki, T., & Akioka, H. (1976). Floristic and distributional account of the common crustose coralline algae on Guam. *Micronesica*, *12*, 247–277.
Guiry, M. D., & Guiry, G. M. (2023). *AlgaeBase*. World-wide electronic publication, National University of Ireland. Retrieved January 13, 2023, from http://www.algaebase.org
Harrington, L., Fabricius, K., De'ath, G., & Negri, A. (2004). Recognition and selection of settlement substrata determine post settlement survival in corals. *Ecology*, *85*, 3428–3437.
Hernandez-Kantun, J. J., Rindi, F., Adey, W. H., Heesch, S., Peña, V., Le Gall, L., & Gabrielson, P. W. (2015). Sequencing type material resolves the identity and distribution of the generitype *Lithophyllum incrustans*, and related European species *L. hibernicum* and *L. bathyporum* (Corallinales, Rhodophyta). *Journal of Phycology*, *51*, 791–800.
Heyward, A. J., & Negri, A. P. (1999). Natural inducers for coral larval metamorphosis. *Coral Reefs*, *18*, 273–279.
Hind, K. R., Gabrielson, P. W., Jensen, C. P., & Martone, P. T. (2016). *Crusticorallina* gen. Nov., a nongeniculate genus in the subfamily Corallinoideae (Corallinales, Rhodophyta). *Journal of Phycology*, *52*, 929–941.
Huelsenbeck, J. P., & Ronquist, F. (2001). MrBayes: Bayesian inference of phylogenetic trees. *Bioinformatics*, *17*, 754–755.
Hughey, J. R., & Gabrielson, P. W. (2012). Comment on "acquiring DNA sequence data from dried archival red algae (Florideophyceae) for the purpose of applying available names to contemporary genetic species: a critical assessment.". *Botany*, *90*, 1191–1194.
Jeong, S. Y., Nelson, W. A., Sutherland, J. E., Peña, V., Le Gall, L., Diaz-Pulido, G., Won, B. Y., & Cho, T. O. (2021). Corallinapetrales and Corallinapetraceae: A new order and family of coralline red algae including *Corallinaptera gabrielii* comb. nov. *Journal of Phycology*, *57*, 849–862.
Johnson, J. H. (1954). An introduction to the study of rock-building algae and algal limestones. *Colorado School of Mines Quarterly*, *49*, 117.
Johnson, J. H. (1961). *Bikini and nearby atolls, Marshall Islands: Fossil calcareous algae from Eniwetok, Funafuti and Kita-Daito-Jima* (Professional Paper 260-Z; pp. 907–950). United States Geological Survey.
Johnson, J. H. (1964). *Fossil and recent calcareous algae from Guam*. (Professional Paper 403-G; pp. 1–40). United States Geological Survey.
Johnson, M. D., & Carpenter, R. C. (2012). Ocean acidification and warming decrease calcification in the crustose coralline alga *Hydrolithon onkodes* and increase susceptibility to grazing. *Journal of Experimental Marine Biology and Ecology*, *434*, 94–101.
Jorissen, H., Galand, P. E., Bonnard, I., Meiling, S., Raviglione, D., Meistertzheim, A.-L., Hédouin, L., Banaigs, B., Payri, C. E., & Nugues, M. M. (2021). Coral larval settlement preferences linked to crustose coralline algae with distinct chemical and microbial signatures. *Scientific Reports*, *11*, 14610.
Kato, A., Baba, M., & Suda, S. (2011). Revision of the Mastophoroideae (Corallinales, Rhodophyta) and polyphyly in nongeniculate species widely distributed on Pacific coral reefs. *Journal of Phycology*, *47*, 662–672.
Kumar, S., Stecher, G., & Tamura, K. (2016). MEGA7: Molecular evolutionary genetics analysis version 7.0. For bigger datasets. *Molecular Biology and Evolution*, *33*, 870–874.
Lanfear, R., Frandsen, P. B., Wright, A. M., Senfeld, T., & Calcott, B. (2016). PartitionFinder 2: New methods for selecting partitioned models of evolution for molecular and morphological phylogenetic analyses. *Molecular Biology and Evolution*, *34*, 772–773.
Lee, Y. P. (2008). *Marine algae of Jeju*. Academy Publication.
Levring, T. (1943). Die Corallinaceen der Juan Fernandez-Inseln [the Corallinaceae of the Juan Fernandez Islands]. In C. Skottsberg (Ed.), *The natural history of Juan Fernandez and Easter Island* (Vol. *2*, pp. 753–757). Almqvist & Wiksells.
Littler, D. S., & Littler, M. M. (2003). *South Pacific reef plants: A diver's guide to the plant life of South Pacific coral reefs*. Offshore Graphics.
Littler, M. M., & Doty, M. S. (1975). Ecological components structuring the seaward edges of tropical pacific reefs: The distribution, communities and productivity of *Porolithon*. *Journal of Ecology*, *63*, 117–129.
Littler, M. M., & Littler, D. S. (2013). The nature of crustose coralline algae and their interaction on reefs. *Smithsonian Contributions to the Marine Sciences*, *39*, 199–212.
Lobban, C. S., & Tsuda, R. T. (2003). Revised checklist of benthic marine macroalgae and seagrasses of Guam and Micronesia. *Micronesica*, *35*(36), 54–99.
Magruder, W. H., & Hunt, J. W. (1979). *Seaweeds of Hawaii: A photographic identification guide*. The Oriental Publishing Company.
Maneveldt, G. W. (2005). *A global revision of the nongeniculate coralline algal genera Porolithon* Foslie *(defunct) and Hydrolithon* Foslie *(Corallinales, Rhodophyta)*. [Doctoral dissertation, University of the Western Cape].
Maneveldt, G. W., Gabrielson, P. W., & Kangwe, J. (2017). *Sporolithon indopacificum* sp. nov. (Sporolithales, Rhodophyta) from tropical western Indian and western Pacific oceans: First report, confirmed by DNA sequence data, of a widely distributed species of *Sporolithon*. *Phytotaxa*, *326*, 115–128.
Maneveldt, G. W., & Keats, D. W. (2014). Taxonomic review based on new data of the reef-building alga *Porolithon onkodes* (Corallinaceae, Corallinales, Rhodophyta) along with other taxa found to be conspecific. *Phytotaxa*, *190*, 216–249.
Maneveldt, G. W., & Keats, D. W. (2016). Taxonomic review based on new morpho-anatomical data of the algae *Porolithon craspedium* and *P. gardineri* (Corallinaceae, Corallinales, Rhodophyta), and comments on other taxa ascribed to the genus. *Phytotaxa*, *289*, 1–35.
Martín, J. M., & Braga, J. C. (1993). Eocene to Pliocene coralline algae in the Queensland plateau (northeastern Australia). *Proceedings of the Ocean Drilling Program, Scientific Results*, *133*, 67–74.
Nash, M. C., Diaz-Pulido, G., Harvey, A. S., & Adey, W. H. (2019). Coralline algal calcification: A morphological and process-based understanding. *PLoS ONE*, *14*, e0221396.
O'Leary, J. K., Barry, J. P., Gabrielson, P. W., Rogers-Bennett, L., Potts, D. C., Palumbi, S. R., & Micheli, F. (2017). Calcifying algae maintain settlement cues to larval abalone following algal exposure to extreme ocean acidification. *Scientific Reports*, *7*, 5774.
Page, T. M., McDougall, C., Bar, I., & Diaz-Pulido, G. (2022). Transcriptomic stability or lability explains sensitivity to climate stressors in coralline algae. *BMC Genomics*, *23*, 729.
Payri, C. E., & Cabioch, G. (2004). The systematics and significance of coralline red algae in the rhodolith sequence of the Amédée 4 drill core (South West New Caledonia). *Palaeogeograpy, Palaeoclimatology, Palaeoecology*, *204*, 187–208.
Payri, C. E., & N'Yeurt, A. D. R. (1997). A revised checklist of Polynesian benthic marine algae. *Australian Systematic Botony*, *10*, 867–910.
Peña, V., Le Gall, L., Rösler, A., Payri, C. E., & Braga, J. C. (2018). *Adeylithon bosencei* gen. et sp. nov. (Corallinales, Rhodophyta): A new reef-building genus with anatomical affinities with the fossil *Aethesolithon*. *Journal of Phycology*, *55*, 134–145.
Penrose, D., & Woelkerling, W. J. (1992). A reappraisal of *Hydrolithon* and its relationship to *Spongites* (Corallinaceae, Rhodophyta). *Phycologia*, *31*, 81–88.
Pezzolesi, L., Peña, V., Le Gall, L., Gabrielson, P. W., Kaleb, S., Hughey, J. R., Rodondi, G., Hernandez-Kantun, J. J., Falace,

A., Basso, D., Cerrano, C., & Rindi, F. (2019). Mediterranean *Lithophyllum stictiforme* (Corallinales, Rhodophyta) is a genetically diverse species complex: Implications for species circumscription, biogeography and conservation of coralligenous habitats. *Journal of Phycology*, *55*, 473–492.
Richards, J. L., Saunders, G. W., Hughey, J. R., & Gabrielson, P. W. (2021). Reinstatement of Indian Ocean *Porolithon coarctatum* and *P. gardineri* based on sequencing type specimens, and *P. epiphyticum* sp. nov. (Corallinales, Rhodophyta), with comments on subfamilies Hydrolithoideae and Metagoniolithoideae. *Botanica Marina*, *64*, 363–377.
Rindi, F., Braga, J. C., Martin, S., Peña, V., Le Gall, L., Caragnano, A., & Aguirre, J. (2019). Coralline algae in a changing Mediterranean Sea: How can we predict their future, if we do not know their present? *Frontiers in Marine Science*, *6*, 723.
Ringeltaube, P., & Harvey, A. (2000). Non-geniculate coralline algae (Corallinales, Rhodophyta) on Heron reef, Great Barrier Reef (Australia). *Botanica Marina*, *43*, 431–454.
Ronquist, F., & Huelsenbeck, J. P. (2003). MrBayes 3: Bayesian phylogenetic inference under mixed models. *Bioinformatics*, *19*, 1572–1574.
Rösler, A., Perfectti, F., Peña, V., Aguirre, J., & Braga, J. C. (2017). Timing of the evolutionary history of Corallinaceae (Corallinales, Rhodophyta). *Journal of Phycology*, *53*, 567–576.
Rösler, A., Pretkovi ć, V., Novak, V., Renema, W., & Braga, J. C. (2015). Coralline algae from the Miocene Mahakam Delta (East Kalimantan, SE Asia). *PALAIOS*, *30*, 83–93.
Santelices, B., & Abbott, I. A. (1987). Geographic and marine isolation: An assessment of the marine algae of Easter Island. *Pacific Science*, *41*, 1–20.
Silva, P. C., Basson, P. W., & Moe, R. L. (1996). *Catalogue of the benthic marine algae of the Indian Ocean*. University of California Press.
Silvestro, D., & Michalak, I. (2012). raxmlGUI: A graphical front-end for RAxML. *Organisms Diversity & Evolution*, *12*, 335–337.
South, G. R., & Skelton, P. A. (2003). Catalogue of the marine benthic macroalgae of the Fiji Islands, South Pacific. *Australian Systematic Botany*, *16*, 699–758.
Stamatakis, A. (2006). RAxML-VI-HPC: Maximum likelihood-based phylogenetic analyses with thousands of taxa and mixed models. *Bioinformatics*, *22*, 2688–2690.
Stamatakis, A., Hoover, P., & Rougemont, J. (2008). A rapid bootstrap algorithm for the RAxML web servers. *Systematic Biology*, *57*, 758–771.
Struck, T. H., Feder, J. L., Bendiksby, M., Birkeland, S., Cerca, J., Gusarov, V. I., Kistenich, S., Larsson, K.-H., Liow, L. H., Nowak, M. D., Stedje, B., Bachmann, L., & Dimitrov, D. (2018). Finding evolutionary processes hidden in cryptic species. *Trends in Ecology & Evolution*, *33*, 153–162.
Taylor, W. R. (1950). *Plants of bikini and other northern Marshall Islands*. University of Michigan Press.
Teichert, S., Steinbauer, M., & Kiessling, W. (2020). A possible link between coral reef success, crustose coralline algae and the evolution of herbivory. *Scientifc Reports*, *10*, 17748.
Thiers, B. (2023). Index Herbariorum: A global directory of public herbaria and associated staff. New York Botanical Garden's Virtual Herbarium. Retrieved January 8, 2023, from http://sweetgum.nybg.org/ih/
Thompson, J. D., Higgins, D. G., & Gibson, T. J. (1994). ClustalW: Improving the sensitivity of progressive multiple sequence alignment through sequence weighting, position-specific gap penalties and weight matrix choice. *Nucleic Acids Research*, *22*, 4673–4680.
Tittley, I., Irvine, L., & Kartawick, T. (1984). *Catalogue of type specimens and geographical index to the collections of Rhodophyta (red algae) at the British Museum (Natural History)*. British Museum (Natural History).
Tsuda, R. T. (2003). Checklist and bibliography of the marine benthic algae from the Mariana Islands (Guam and CNMI). *University of Guam Marine Laboratory Technical Reports*, *107*, 1–49.
Tsuda, R. T., & Fisher, J. R. (2012). Floristic account of the marine benthic algae from Jarvis Island and Kingman reef, Line Islands, Central Pacific. *Micronesica*, *43*, 14–50.
Tsuda, R. T., & Walsh, S. K. (2013). Bibliographic checklist of the marine benthic algae of Central Polynesia in the Pacific Ocean (excluding Hawai'i and French Polynesia). *Micronesica*, *2013*, 1–91.
Verheij, E. (1994). Nongeniculate Corallinaceae (Corallinales Rhodophyta) from the Spermonde archipelago, SW Sulawesi, Indonesia. *Blumea*, *39*, 95–137.
Vieira, C., N'Yeurt, A. D. R., Rasoamanendrika, F. A., D'Hondt, A., Thi Thram, L. A., Van de Spiegel, S., Kawai, H., & De Clerck, O. (2021). Marine macroalgal biodiversity of norther Madagascar: Morpho-genetic systematics and implications of anthropic impacts for conservation. *Biodiversity and Conservation*, *30*, 1501–1546.
Woelkerling, W. J. (1993). Type collections of Corallinales (Rhodophyta) in the Foslie herbarium (TRH). *Gunneria*, *67*, 1–289.
Woelkerling, W. J. (1998). Type collections of non-geniculate corallines housed at the Laboratoire de Cryptogamie (PC). In W. J. Woelkerling & D. Lamy (Eds.), *Non-geniculate coralline red algae and the Paris museum: Systematics and scientific history*. Muséum National d'Histoire Naturelle [National Museum of Natural History]/ADAC.
Yoon, H. S., Hackett, J. D., & Bhattacharya, D. (2002). A single origin of the peridinin- and fucoxanthin-containing plastids in dinoflagellates through tertiary endosymbiosis. *Proceedings of the National Academy of Sciences*, *99*, 11724–11729.

SUPPORTING INFORMATION

Additional supporting information can be found online in the Supporting Information section at the end of this article.

Table S1. List of specimen information used in molecular analyses.

How to cite this article: Jeong, S. Y., Gabrielson, P. W., Hughey, J. R., Hoey, A. S., Cho, T. O., Abdul Wahab, M. A., & Diaz-Pulido, G. (2023). New branched *Porolithon* species (Corallinales, Rhodophyta) from the Great Barrier Reef, Coral Sea, and Lord Howe Island. *Journal of Phycology*, *00*, 1–23. https://doi.org/10.1111/jpy.13387